

Temporally-Evolving Generalised Networks and their Reproducing Kernels

Tobia Filosi¹, Claudio Agostinelli¹, and Emilio Porcu^{2,3}

¹Department of Mathematics, University of Trento, Italy

²Department of Mathematics, Khalifa University, Abu Dhabi,
UAE

³School of Computer Science and Statistics, Trinity College
Dublin, Ireland

September 29, 2023

Abstract

This paper considers generalised network, intended as networks where (a) the edges connecting the nodes are nonlinear, and (b) stochastic processes are continuously indexed over both vertices and edges. Such topological structures are normally represented through special classes of graphs, termed graphs with Euclidean edges. We build generalised networks in which topology changes over time instants. That is, vertices and edges can disappear at subsequent time instants and edges may change in shape and length. We consider both cases of linear or circular time. For the second case, the generalised network exhibits a periodic structure. Our findings allow to illustrate pros and cons of each setting. Generalised networks become semi-metric spaces whenever equipped with a proper semi-metric. Our approach allows to build proper semi-metrics for the temporally-evolving topological structures of the networks. Our final effort is then devoted to guiding the reader through appropriate choice of classes of functions that allow to build proper reproducing kernels when composed with the temporally-evolving semi-metrics topological structures.

Keywords — Generalised networks, time-evolving graphs, reproducing kernels, semi-metric spaces.

1 Introduction

1.1 Context

Data complexity is certainly one of the main aspects to address in the Data Science revolution framework. In particular, we call *3D* complexities those aspects related to Data structure, Data dimension and Data domain. The present paper concerns the latter of these aspects and delves into the problem of graphs whose nodes and edges evolve dynamically over time.

Data analysis on graphs became ubiquitous in both Statistics and Machine Learning communities. For the first, recent contributions as in [Anderes et al. \[2020\]](#), [Moradi and Mateu \[2020\]](#), [Baddeley et al. \[2021\]](#) and [Rakshit et al. \[2017\]](#) witness the importance of graph structures for georeferenced data, being realisations of either geostatistical or point processes. As for the machine learning community, the amount of literature is huge. Open Graph Benchmark (OGB) is a comprehensive set of challenging and realistic benchmark datasets with the aim to facilitate scalable, robust and reproducible graph machine learning (ML) research [[Hu et al., 2020](#)]. An overview of ML methodological approaches on graphs is provided by [Chami et al. \[2022\]](#). Topological complexities under the framework of data analytics are discussed in [Stanković et al. \[2020\]](#). Excellent surveys about ML on graphs are oriented to angles as different as large scale challenges [[Hu et al., 2021](#)], automated ML [[Zhang et al., 2021](#)], representation learning [[Hamilton et al., 2017](#)], relational ML for knowledge graphs [[Nickel et al., 2015](#)] and higher order learning [[Agarwal et al., 2006](#)], to mention just a few.

In the great majority of contributions, the process is assumed to be defined exclusively over the vertices of the graph. The extension to processes that are continuously defined over both graphs and edges requires substantial mathematical work.

This paper focuses on graphs with Euclidean edges [[Anderes et al., 2020](#)], being an ingenious topological structure that allows to generalise linear networks to nonlinear edges. Further, the process defined over such structures can have realisations over any point over the edges, and not only in the nodes. Roughly, these are graphs where each edge is associated with an abstract set in bijective correspondence with a segment of the real line. This provides each edge with a Cartesian coordinate system to measure distances between any two points on that edge.

There has been increasing attention on generalised networks in ML [[Al-](#)

sheikh et al., 2014, Georgopoulos and Hasler, 2014, Hamilton et al., 2017, Pinder et al., 2021, Borovitskiy et al., 2022], spatial data [Cressie et al., 2006, Gardner et al., 2003, Ver Hoef et al., 2006, Peterson et al., 2013, 2007, Montembeault et al., 2012] and point processes [Xiao et al., 2017, Perry and Wolfe, 2013, Deng et al., 2014, Baddeley et al., 2017]. For all these contributions, *time* is not part of the game.

Reproducing kernel Hilbert space (RKHS) methods [Hofmann et al., 2008] had a considerable success in both ML and Statistics community, and the reader is referred to Hofmann et al. [2006], Kung [2014] and to Pillonetto et al. [2014] for excellent overviews.

RKHS methods require *kernels*, being positive semidefinite functions defined over a suitable input space. A customary assumption for such kernels is that of isotropy, *i.e.* the kernel depends only on the distance between any pair of points belonging to the input space. There is a rich literature at hand for the case of the input space being a d -dimensional Euclidean space [see the celebrated work of Schoenberg, 1942], and the reader is referred to the recent review by Porcu et al. [2023a]. Non Euclidean domains have a more recent literature, and we mention Porcu et al. [2016] as well as Borovitskiy et al. [2023] and Borovitskiy et al. [2021] for recent contributions. For such cases, the *distance* between the points is no longer the Euclidean distance, but the geodesic distance.

The *tour de force* by Anderes et al. [2020] has allowed to define isotropic reproducing kernels for generalised network, by working with two metrics: the geodesic and the resistance metric. Elegant isometric embedding arguments therein allow to provide sufficient conditions for given classes of functions to generate a legitimate reproducing kernel through composition with either of the two metrics. See the discussion in Section 2.

1.2 Graphs cross time and temporally-evolving graphs

Data on generalised networks are usually repeatedly observed over time. For such a case, it is customary to consider the input space, X , as a product (semi) metric space, with two separate metrics: the geodesic (or the resistance) metric for the graph, and the temporal separation for time. This approach has considerable advantages as it simplifies the mathematical architecture considerably. Unfortunately, under such a setting, the graph topology is invariant over time. This fact implies that nodes cannot disappear (nor new nodes can appear at arbitrary future instant times), and the shape and

length of the edges do not evolve over time. Reproducing kernels for such a case have been recently proposed by [Porcu et al. \[2023b\]](#) and by [Tang and Zimmerman \[2020\]](#). When the input space is a product space equipped with separate metrics, the kernel is component-wise isotropic when it depends, on the one hand, on a suitable distance over the graph and, on the other hand, on temporal separation. For details, the reader is referred to [Porcu et al. \[2023b\]](#). For the case of static metric graphs, we mention the impressive approach in [Bolin and Lindgren \[2011\]](#).

Outside the reproducing kernel framework, scientists have been mainly focused on the topological structure of temporally dynamical networks [[Hanneke et al., 2010](#)]. This fact boosted for a wealth of related approaches, ranging from community detection methods [[Mankad and Michailidis, 2013](#), [Cherifi et al., 2019](#)] to link prediction [[Lim et al., 2019](#), [Divakaran and Mohan, 2020](#)] to structural changes detection [[Rossi et al., 2013](#)]. The common feature of the above contributions is that they consider the stochastic evolution of the structure (nodes and edges) of the graphs as the basis for the inference, whilst they do not usually allow for *processes* defined over those graphs.

1.3 Linear or circular time? Might graphs be periodic?

This paper consider time-evolving graphs. While the choice of linear time does not need any argument—this is what most of the literature does—this paper argues that periodically-evolving graphs have a reason to exist. Our first argument to advocate in favour of a periodic construction is that it suits perfectly to several real-world phenomena, where both linear-time evolution (*e.g.* long-term trends) and cyclic oscillations (*e.g.* seasonal components) might happen. To make an example, consider temperatures in a given geographical area: apparently there might be strong correlations between: (i) contiguous spatial points at a given time, which are represented by means of spatial edges; (ii) the same points considered at contiguous times, which are represented by means of temporal edges between temporal layers and (iii) the same points considered at the same periods of the year, which are considered in the model as they are exactly the same point in the temporally evolving graph. In many real-world applications, the network underlying a system is only partially observable. As a consequence, it could be hard or impossible to specify the whole time-evolving (not periodic) network in cases of long time series. The periodic assumption, when all in all reasonable, may be a

great help in this circumstance as well.

1.4 Our contribution

This paper provides the following contributions.

1. We provide a mathematical construction for graphs with Euclidean edges having a topology that evolves over time. That is, the number of vertices can change over time, as well as the shape and length of the edges. Remarkably, our construction allows for stochastic processes that are continuously indexed over both vertices and edges.
2. We start by considering the case of linear time. After providing the structure for a temporally evolving graph, we devote substantial mathematical effort to build a suitable semi-metric over it. This is achieved at the expense of a sophisticated construction through a Gaussian bridge that is interpolated through the edges in the spatio-temporal domain.
3. As an implication of the previous points, we obtain suitable second order properties (hence, the reproducing kernel) associated with such a process.
4. The previous steps are then repeated for a periodic time-evolving graph.
5. We prove that the construction with linear time might have a counterintuitive property: adding temporal layers can change the inter-space distances between points in the graph. This might be a problem in terms of statistical inference, as carefully explained through the paper. We show that the periodic construction does not present such an inconvenience.
6. Our findings culminate by guiding the reader through handy constructions for kernels defined over these graphs.

We should mention that our contribution differentiates with respect to earlier literature in several directions. In particular:

1. We allow the topology of the graph to evolve over time (whatever linear or circular). Previous contributions where graphs with Euclidean edges are considered use either a static graph [[Anderes et al., 2020](#), [Bolin](#)

et al., 2022] or a graph having a topology that is invariant with respect to time [Porcu et al., 2023b, Tang and Zimmerman, 2020]. Hence, we provide a very flexible framework in comparison with earlier literature.

2. We allow stochastic processes to be continuously defined over the graph. This is a substantial innovation with respect to a massive literature from both Statistics and ML, where the graph topology can vary according to some probability law associated with the nodes, but not to processes defined over the nodes.

The structure of the paper is the following. Section 2 recalls the main mathematical objects that will be used. Section 3 builds the skeleton of our construction, *i.e.* time-evolving graphs, which are exploited in Sections 4 and 5, where time-evolving graphs with Euclidean edges are defined for the linear time and circular time cases, respectively. Section 6 illustrates how it is possible to build kernels on such a structure and present some examples. Finally, Section 7 concludes the paper.

In addition, in Appendix A we recall some mathematical definitions used throughout. In Appendix B, we recall and then extend some significant results by Anderes et al. [2020] about the definition of kernels on arbitrary domains that are used in this manuscript, and present them under a general and easy-to-handle perspective. As proofs are rather technical, we defer them to Appendix C for a neater exposition of the main text.

2 Mathematical background

This material is largely expository and provides the necessary mathematical background needed to understand the concept illustrated in the main text. For the unfamiliar reader, Appendix A provides basic definitions and concepts used in network theory.

2.1 Gaussian random fields over semi-metric spaces

Let us begin with a brief introduction about Gaussian random fields [Stein, 1999]

Let X be a non-empty set and let $k : X \times X \rightarrow \mathbb{R}$. Then k is a *positive semi-definite* function (or a *kernel*, or a *covariance function*) if and only if,

for all $n \in \mathbb{N}^+$, $x_1, \dots, x_n \in X$ and $a_1, \dots, a_n \in \mathbb{R}$,

$$\sum_{i=1}^n \sum_{j=1}^n a_i a_j k(x_i, x_j) \geq 0. \quad (1)$$

If, in addition, whenever the above relation is an equality, then necessarily $a_1 = \dots = a_n = 0$, k is (*strictly*) *positive definite*.

For X as above, we denote Z a real-valued random field, *videlicet*: for each $x \in X$, $Z(x)$ is a real-valued random variable. Then Z is called *Gaussian* if, for all $n \in \mathbb{N}^+$ and $x_1, \dots, x_n \in X$, the random vector $\mathbf{Z} := (Z(x_1), \dots, Z(x_n))^\top$, with \top denoting the transpose operator, follows a n -variate Gaussian distribution.

A Gaussian random field Z on X is completely determined by its first two moments: the mean function

$$\begin{aligned} \mu_Z : X &\rightarrow \mathbb{R} \\ x &\mapsto \mathbb{E}(Z(x)), \end{aligned}$$

with \mathbb{E} denoting stochastic expectation, and the covariance function (kernel)

$$\begin{aligned} k_Z : X \times X &\rightarrow \mathbb{R} \\ (x_1, x_2) &\mapsto \text{Cov}(Z(x_1), Z(x_2)). \end{aligned}$$

A necessary and sufficient condition for a function k_Z to be a covariance function (a kernel) of some random field Z is to be positive semi-definite.

For X as above, we define a mapping $d : X \times X \rightarrow \mathbb{R}$. Then (X, d) is called *semi-metric space* (or, equivalently, d is called a *semi-metric* on X) if the following conditions hold for each $x, y \in X$:

1. $d(x, y) \geq 0$,
2. $d(x, y) = 0 \iff x = y$,
3. $d(x, y) = d(y, x)$.

In addition, (X, d) is called a *metric space* (or, equivalently, d is called a *metric* on X) if it is a semi-metric space and the triangle inequality holds, namely, for all $x, y, z \in X$:

$$d(x, y) + d(y, z) \geq d(x, z).$$

The covariance function k_Z is called isotropic for the semi-metric space (X, d) if there exists a mapping $\psi : D_X^d \rightarrow \mathbb{R}$ such that $k_Z(x, y) = \psi(d(x, y))$, for $x, y \in X$. Here, $D_X^d := \{d(x_1, x_2) : x_1, x_2 \in X\}$ is the diameter of X . See Appendix B on how to construct isotropic kernels on arbitrary domains. For a Gaussian random field Z on X , we define its *variogram* $\gamma_Z : X \times X \rightarrow \mathbb{R}$ through

$$\gamma_Z(u_1, u_2) := \text{Var}(Z(u_1) - Z(u_2)), \quad u_1, u_2 \in X, \quad (2)$$

with Var denoting *variance*. The celebrated work of Schoenberg [1942] proves that γ_Z is a variogram if and only if the mapping $\exp(-\gamma_Z(\cdot, \cdot))$ is positive definite on $X \times X$.

Let (X_1, d_1) and (X_2, d_2) be two semi-metric spaces. Then, the triple $(X_1 \times X_2, d_1, d_2)$ is called a *product semi-metric space*. Menegatto et al. [2020] define isotropy over a product semi-metric space through continuous functions $\psi : D_{X_1}^{d_1} \times D_{X_2}^{d_2} \rightarrow \mathbb{R}$ such that, for $(x_1, x_2), (x'_1, x'_2) \in X_1 \times X_2$,

$$((x_1, x_2), (x'_1, x'_2)) \mapsto \psi(d_1(x_1, x'_1), d_2(x_2, x'_2)), \quad (3)$$

is positive definite.

The above definition naturally arises from spatio-temporal settings: suppose we have a *static* semi-metric space (X, d) that represents some spatial structure and (T, d_T) representing time, where $T \subseteq \mathbb{R}$ and, usually, $d_T(t_1, t_2) = |t_1 - t_2|$. In such a case, Equation (3) can be re-adapted to define kernels. This is the setting adopted by Porcu et al. [2023b] and by Tang and Zimmerman [2020].

Remark 1. We deviate from earlier literature and we instead consider a metric space X_t that evolves over time, $t \in T$. Hence, our domain is written as

$$\{(x_t, t) : x_t \in X_t, t \in T\},$$

where t describes *time*, and the graph coordinate x_t is constrained on the space X_t . Such a framework entails a way more sophisticated construction to equip such a space with a proper metric.

2.2 Graphs with Euclidean edges

We start with a formal definition of graphs with Euclidean edges. We slightly deviate from the definition provided by Anderes et al. [2020], for the reasons that will be clarified subsequently. For a definition of graph, see 5 in the Appendix.

Definition 1 (Graph with Euclidean edges). Consider a simple, connected and weighted graph $G = (V, E, w)$, where $w : E \rightarrow \mathbb{R}^+$ represents the weight mapping. Then, G is called a *graph with Euclidean edges* provided that the following conditions hold.

1. Edge sets: Each edge $e \in E$ is associated to the compact segment (also denoted by e) $[0, \ell(e)]$, where $\ell(e) := w(e)^{-1}$ may be interpreted as the *length* of the edge e .
2. Linear edge coordinates: Each point $u \in e = (\underline{u}, \bar{u})$ is uniquely determined by the endpoints \underline{u} and \bar{u} of e and its relative distance $\delta_e(u) := \frac{u}{\ell(e)} = u w(e)$ from \underline{u} , that is $u = (\underline{u}, \bar{u}, \delta_e(u))$, so that $\underline{u} = (\underline{u}, \bar{u}, 0) = (\bar{u}, \underline{u}, 1)$ and $\bar{u} = (\underline{u}, \bar{u}, 1) = (\bar{u}, \underline{u}, 0)$.

Henceforth, we shall assume the existence of a total order relation on the set of vertices V and that every edge is represented through the ordered pair (v_1, v_2) , where $v_1 < v_2$. In particular, for each $u \in e$, the endpoints of e , \underline{u} and \bar{u} satisfy the relation $\underline{u} < \bar{u}$.

A relevant fact is that our setting deviates from [Anderes et al. \[2020\]](#). In particular, our Definition 1 does not require any *distance consistency* opposed to [Anderes et al. \[2020, Definition 1, \(d\)\]](#). The reason is that our setting does not need a bridge between geodesic and resistance metrics. A second relevant fact is that we have restricted the space of possible bijections from each edge onto closed intervals with orientation. We restrict to linear bijections: the main reason is that the focus of this paper is not to explore isometric embeddings, but to provide suitable topological structures evolving over time, and attach to them stochastic processes.

As a final remark, we stress that the framework introduced through Definition 1 is way more general than linear networks, for at least two reasons: (a) in our framework, the weights of each edge be chosen independently from the others, and (b) our framework needs no restriction on the network structure, *e.g.*, as shown in Figure 1 (right), edges may cross without sharing the crossing point.

2.3 Graph laplacian and resistance metric

The resistance metric has been widely used in graph analysis, as it is more natural than the shortest-path metric when considering flows or transport networks, where multiple roads between two given points may share the

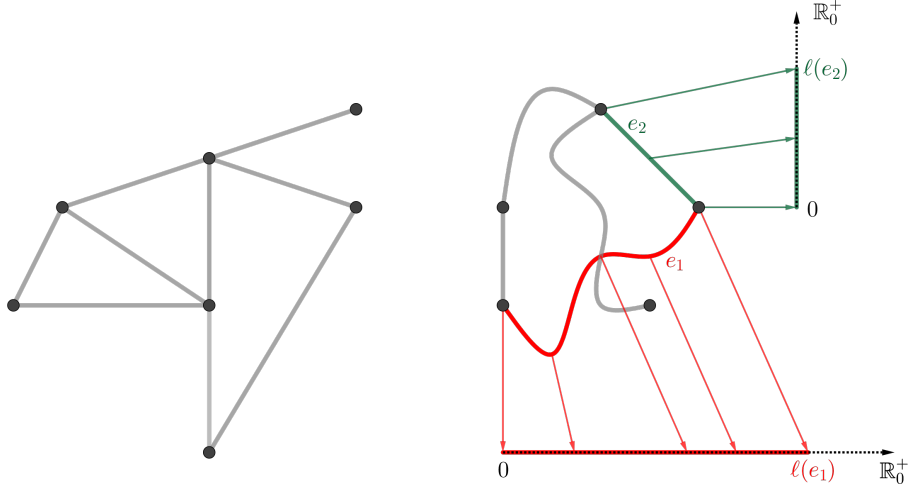


Figure 1: Left: a linear network. Right: a graph with Euclidean edges, where the bijections between the edges e_1 and e_2 and their respective real segments $[0, \ell(e_1)]$ and $[0, \ell(e_2)]$ are stressed.

total flow. In order to define the classic effective resistance distance for an undirected and connected graph, we briefly report its definition and its mathematical construction.

Let $G = (V, E, w)$ be a simple, weighted and connected graph (see Definition 5 in the Appendix) and let W its adjacency matrix, that is: $W(v_1, v_2) = w((v_1, v_2))$, where we set $w((v_1, v_2)) = 0$ whenever $v_1 \not\sim v_2$. In addition, for each node $v \in V$, we define its *degree* as the sum of the weights of the edges adjacent to it. Let D be the degree matrix of G , i.e. the diagonal matrix where each diagonal element is the degree of the corresponding vertex. Then, the *laplacian matrix* (or simply *laplacian*) of G is the matrix $L := D - W$, namely the matrix $L : V \times V \rightarrow \mathbb{R}$ having entries

$$L(v_1, v_2) = \begin{cases} -w((v_1, v_2)) & \text{if } v_1 \neq v_2 \\ \sum_{u \in V} w((v_1, u)) & \text{if } v_1 = v_2. \end{cases} \quad (4)$$

Laplacian matrices enjoy several properties (see, for instance, Devriendt [2022]): they are symmetric, diagonally dominant, positive semidefinite and singular with exactly one null eigenvalue, corresponding to the eigenvector

$\mathbf{1}_n$. Furthermore, they have non-positive off-diagonal entries and positive main-diagonal entries.

A graph $G = (V, E)$ is called a *resistor graph* if the edges $e \in E$ represent electrical resistors and the nodes represent contact points. Given a resistor graph, the *effective resistance distance* R between two vertices is defined as the voltage drop between them when injecting one Ampere of current in one and withdrawing one Ampere from the other.

Several mathematical formulations of this concept have been provided, and the reader is reminded, among many others, to [Jorgensen and Pearse \[2010, Subsection 2.1\]](#). Throughout, we follow [Ghosh et al. \[2008\]](#). Let $G = (V, E)$ be a resistor graph. For each $v_1 \sim v_2 \in V$, let $r(v_1, v_2) \in \mathbb{R}^+$ denote the resistance of the resistor that connects v_1 and v_2 . In addition, for each $v_1, v_2 \in V$, define the weight (which plays the role of the physical conductance)

$$w((v_1, v_2)) := \begin{cases} \frac{1}{r((v_1, v_2))} & \text{if } v_1 \sim v_2 \\ 0 & \text{if } v_1 \not\sim v_2. \end{cases}$$

Let L be the laplacian matrix of G with the above-defined weights, L^+ its Moore-Penrose generalised inverse (see Definition 6 in the Appendix). Finally let e_{v_i} denote the vector with all zeroes, except a one at position v_i . Then the effective resistance distance R between two nodes v_1 and v_2 enjoys the following expression:

$$R(v_1, v_2) = (e_{v_1} - e_{v_2})^\top L^+ (e_{v_1} - e_{v_2}). \quad (5)$$

3 Time-evolving graphs with Euclidean edges

Defining a time-evolving graph with Euclidean edges requires some mathematical formalism. While keeping such a formalism below, we shall then provide some narrative in concert with some graphical representation to have an intuition of how these graphs work.

Even though the underlying rationale of our construction is quite natural and intuitive, the mathematical description of such an object is quite involved as it requires several of steps and a substantial formalism. Hence, we provide a sketch of our procedure to help the reader in the Box below.

A sketch of our construction

1. Define a time-evolving graph as a properly defined sequence of graphs indexed by discrete time instants;
2. Define *connected equivalent simple* time-evolving graphs by completing a time evolving graph through a set of edges that connect the same nodes at different time instants;
3. Over the connected equivalent simple graph, we can now define, for every time t , a graph with Euclidean edges, G_t ;
4. Define a time-evolving Markov graph to exploit computational advantages.

Some comments are in order. Step 1 is completely general and does not require any topological structure on every *marginal* graph G_t , for a given time t . Yet, having graphs with Euclidean edges that evolve over time requires some more work, and this fact justifies Step 2, which allows for connectivity, being one of the properties *sine qua non* of a graph with Euclidean edges. Step 4 is not mathematically necessary to guarantee the validity of the structure, but it is justified by computational and intuitive reasons as explained throughout.

Step 1 starts with a formal definition.

Definition 2 (Time-evolving graph). Let $T = \{0, \dots, m - 1\}$ be a (finite) collection of time instants. To every time instant $t \in T$ we associate a simple undirected and weighted graph $G_t = (V_t, E_t, w_t)$, with $V_t \cap V_{t'} = \emptyset$ whenever $t \neq t'$. For an edge $e_t \in E_t$, the corresponding weight is denoted $w(e_t) := w_t(e_t)$. We use $n_t := |V_t|$ for the number of vertices at time t .

Let $G = \{G_0, \dots, G_{m-1}\}$ be the associate finite collection of these graphs. Call $V := \bigcup_t V_t$ the set of vertices, $n := |V|$ the total number of vertices, and $E_S := \bigcup_t E_t$ the set of *spatial* edges. Finally, if $v \in V$, whenever convenient we shall write $t(v)$ for the unique value t such that $v \in V_t$.

Let $s : V \rightarrow S$ be a mapping from V , where S is a set of labels, such that $s(v_1) \neq s(v_2)$ whenever v_1 and v_2 are two distinct vertices belonging to the same graph G_t , $t \in T$. Two vertices $v_1 \neq v_2 \in V$ are considered the same vertex at different times if $s(v_1) = s(v_2)$.

We call the triple $\mathbf{G} = (T, G, s)$ a *time-evolving graph*.

While Definition 2 provides a flexible framework to manage graphs that evolve over time, we are going to merge its underlying idea with the one of graph with Euclidean edges presented in Subsection 2.2. Step 2 of our routine intends to *complete* the time-evolving graph as in Definition 2 so to ensure spatio-temporal connectivity.

Let \mathbf{G} be a time-evolving graph. We define its *equivalent simple* time-evolving graph, $\tilde{\mathbf{G}} = (V, \tilde{E})$ as the graph with edges $\tilde{E} := E_S \cup E_T$, with E_T a set of additional edges (called *temporal* edges throughout) that connect the same nodes at different time instants. More precisely, E_T is a subset of $\{(v_1, v_2) \in V \times V : s(v_1) = s(v_2), t(v_1) \neq t(v_2)\}$. To each new edge $e = (v_1, v_2) \in E_T$ a weight $w(e) > 0$ is assigned, while all the other weights remain unchanged. One possibility is to choose $w(e) := \alpha |t(v_1) - t(v_2)|^{-1}$, with $\alpha > 0$ a given scale factor. Although we assume this particular expression in all the following examples, we stress that any choice leads to a valid model as long as $w(e) > 0$.

The intuitive idea behind the construction of an equivalent simple time-evolving graph is to consider m layers, each representing a different temporal instant (namely a graph G_t), and connect them by means of additional intra-time edges, which account for the time-dependency of the graphs. Figure 2 depicts an example of time-evolving graph and the resulting equivalent simple graph. Henceforth, we will consider each connected component of the equivalent simple graph separately.

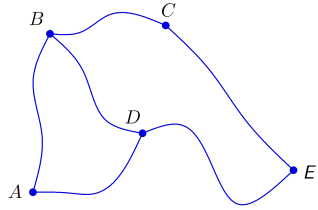
Step 2 ensures that it becomes feasible to assign, to each temporal label $t \in T$, a graph with Euclidean edges to the equivalent simple graph associated with a given time-evolving graph (Step 3). We note that the choice of the temporal edges needs care. Indeed, the set of possible temporal edges for a fixed label $s \in S$ may grow quadratically in the number of considered temporal instants m .

Our proposal is to connect every node that exists at adjacent times, so that there will be no temporal edge connecting non-adjacent times. Hence, we propose a temporally Markovian structure for the graph (Step 4). This is formalised below.

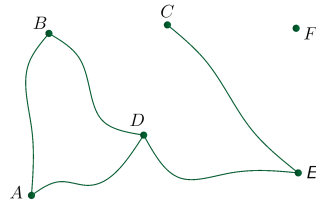
Definition 3 (Time-evolving Markov graph). A *time-evolving Markov graph* is a time-evolving graph $\mathbf{G} = (V, E)$, where

$$E_T \subseteq \{(v_1, v_2) \in V \times V : s(v_1) = s(v_2), |t(v_1) - t(v_2)| = 1\}. \quad (6)$$

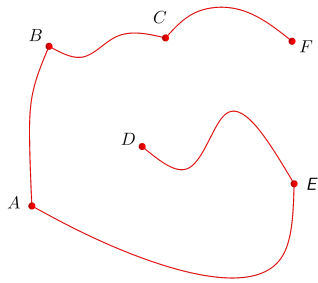
We stress that temporal Markovianity is not needed to prove the mathematical results following subsequently, which work even for the case of non



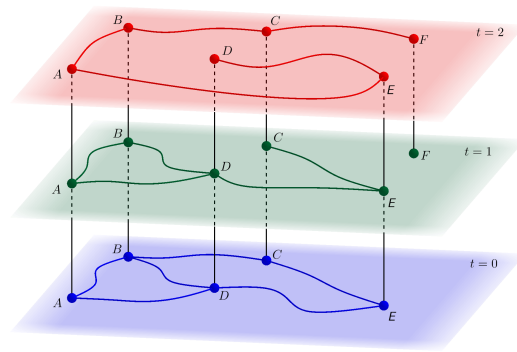
(a) Graph at $t = 0$.



(b) Graph at $t = 1$.



(c) Graph at $t = 2$.



(d) Equivalent simple graph.

Figure 2: An example of an equivalent simple graph (bottom-right), with $m = 3$, $S = \{A, B, C, D, E, F\}$, $n_1 = 5$, $n_2 = n_3 = 6$. The coloured edges belong to E_S , whilst the black ones belong to E_T . The temporal *slices* at time instants $t = 0, 1, 2$ are reported, respectively, at quadrants (a), (b) and (c).

adjacent layers.

Yet, Markovianity simplifies our job considerably. In fact, it allows for a plain representation of an equivalent simple graph. Furthermore, there are non-negligible computational reasons. Indeed, for large networks, Markovianity allows for sparse Laplacian matrices (block tridiagonal) of the associated equivalent simple graph. This entails huge computational savings in both terms of storage and computation. Finally, allowing edges between non-adjacent layers could lead to a huge number of weights α 's. In particular, under the assumption of temporally homogeneous weights (the weight of a temporal edges depends only on the temporal distance between the layers it connects), we would have $m - 1$ possible weights if Markovianity is not assumed. For a large collection of time instants, this can become computationally unfeasible.

We call a time-evolving Markov graph \mathbf{G} *temporally complete* when the set E_T is identically equal to the set in the right hand side of (6). Albeit such a property is not required to prove our theoretical results, it is operationally useful as it allows to avoid removing or adding temporal edges.

4 Resistance metrics for linear time

We start this section by noting that defining the classical resistance metrics between nodes of the temporally evolving graph is not an issue. Yet, we are dealing with a graph where distances should be computed between any pair of points lying continuously over the edges. This is a major challenge that requires some work as follows.

For the case of static graphs with Euclidean edges, [Anderes et al. \[2020\]](#) provide an ingenious construction that allows for a suitable continuously-defined metric on the basis of Brownian bridges and their variograms.

The idea is to follow a similar path, by defining a Gaussian process that is continuously indexed over the edges of an equivalent simple connected graph associated with a given time-evolving graph.

Before going into technical details, we present a brief outline. Following [Anderes et al. \[2020\]](#), we are going to define a distance on all the points of the graph, namely its vertices and the points on its edges. To this aim, we define a Gaussian process Z on every point of the time-evolving equivalent simple Markovian graph and then *define* the distance between two points as

the variogram of such process, i.e., for each $u_1, u_2 \in \tilde{\mathbf{G}}$:

$$d(u_1, u_2) := \gamma_Z(u_1, u_2), \quad (7)$$

with γ_Z as being defined through (2). In such a way, we can directly apply Theorem 1 stated in Appendix B to obtain kernels. Here, $Z := Z_V + Z_E$ is the sum of two independent Gaussian processes defined on the equivalent simple graph $\tilde{\mathbf{G}}$. The process Z_V accounts for the structure of the graph (namely its vertices and the weights of its edges) and plays the role of major source of variability (i.e., the distance), whilst Z_E adds some variability on the edges and accounts for the temporal relationship between the same edge at different times.

4.1 Formal construction of Z_V and Z_E

We start by defining the process Z_V through

$$Z_V(u) := (1 - \delta_e(u)) Z_V(\underline{u}) + \delta_e(u) Z_V(\bar{u}), \quad (8)$$

where $u = (\underline{u}, \bar{u}, \delta_e(u))$, with $e = (\underline{u}, \bar{u})$ and $\delta_e(u)$ as in Definition 1. Further, at the vertices of $\tilde{\mathbf{G}}$, Z_V is defined as a multivariate normal random variable, denoted $Z_V|_V \sim \mathcal{N}(0, L^+)$, being L the laplacian matrix associated to the graph $\tilde{\mathbf{G}}$. The intuitive interpretation is that outside the vertices the process Z_V is obtained through a sheer linear interpolation.

The construction of Z_E is a bit more complex, as Z_E is piecewise defined on a suitable partition of E . A formalisation of this concept follows.

For each $e = (v_1, v_2) \in E_S$, we define the *lifespan* of e , written $\text{ls}(e)$, as the maximal connected set of time instants, t , for which the edge e exists. More formally, $\text{ls}(e)$ is defined as the maximal (with respect to the inclusion partial order) subset of T such that:

- $t(v_1) \in \text{ls}(e)$;
- $\text{ls}(e)$ is connected, that is $\forall t_1 < t_2 \in \text{ls}(e), \{t_1, \dots, t_2\} \subseteq \text{ls}(e)$;
- $\forall t \in \text{ls}(e)$, there exists $(v'_1, v'_2) \in E_S$ such that $s(v'_1) = s(v_1)$, $s(v'_2) = s(v_2)$ and $t(v'_1) = t(v'_2) = t$.

Figure 2 allows to visualise the situation. The lifespan of the edge (A, B) at time $t = 0$ is $\{0, 1, 2\}$; the lifespan of (C, E) at time $t = 1$ is $\{0, 1\}$ and the one of (B, C) at time $t = 2$ is $\{2\}$.

We now define the *life* of e (denoted $\text{lf}(e)$) as the set of edges that represent e at different times and have the same lifespan $\text{ls}(e)$. Formally, we have

$$\text{lf}(e) := \{(v'_1, v'_2) \in E_S : s(v'_1) = s(v_1), s(v'_2) = s(v_2), t(v'_1) = t(v'_2) \in \text{ls}(e)\}.$$

For convenience, we define the life for temporal edges as well: if $e \in E_T$, $\text{lf}(e) := \{e\}$.

It is clear that the set $\{\text{lf}(e) : e \in E_S\}$ forms a partition of all the spatial edges E_S , and that $\{\text{lf}(e) : e \in E_T\}$ is a partition of E_T . The main idea is to consider the life of each spatial and temporal edge and define a suitable process on it, being independent from the others.

Let us consider a spatial edge $e \in E_S$ and its lifespan $\text{ls}(e)$. Consider now the set $\text{ls}(e) \times [0, 1]$ and define on it a zero-mean Gaussian process $B(t, \delta)$ whose covariance function is given by

$$k_B((t_1, \delta_1), (t_2, \delta_2)) := k_T(|t_1 - t_2|) k_{BB}(\delta_1, \delta_2), \quad (9)$$

with $t_1, t_2 \in \text{ls}(e)$ and $\delta_1, \delta_2 \in [0, 1]$. Here k_T is a temporal kernel defined on \mathbb{N} such that $k_T(0) = 1$ and $k_{BB}(\delta_1, \delta_2) := \min(\delta_1, \delta_2) - \delta_1\delta_2$ is the kernel of the standard Brownian bridge on $[0, 1]$. Notice that the spatial marginals of the process B are standard Brownian bridges. We stress that the process $B(t, \delta)$ is only needed for the definition of the process Z_E on $\text{lf}(e)$, as it is better explained below. Now, we define the process Z_E on $\text{lf}(e)$, denoted $Z_E|_{\text{lf}(e)}$, as follows: given an edge $e' = (\underline{u}, \bar{u}) \in \text{lf}(e)$ and given a point $u = (\underline{u}, \bar{u}, \delta)$ on it,

$$Z_E|_{\text{lf}(e)}(u) := \sqrt{\ell(e')} B(t(\underline{u}), \delta). \quad (10)$$

Finally, for each temporal edge $e = [0, \ell(e)] \in E_T$, we define the process Z_E on it as an independent (from both Z_V and Z_E on E_S) Brownian bridge on $[0, \ell(e)]$, having covariance function given by

$$\text{Cov}(Z_E|_e(\delta_1), Z_E|_e(\delta_2)) = \ell(e) (\min(\delta_1, \delta_2) - \delta_1\delta_2).$$

This concludes the construction of the process on the whole set of the edges.

4.2 Mathematical properties of the construction

We remind the reader that the process Z is Gaussian, being the sum of two independent Gaussian processes. Hence, the finite dimensional distribution

of Z is completely specified through the second order properties, namely the covariance function. The following result provides an analytical expression for the covariance function associated with Z .

Proposition 1. *Let $u_1, u_2 \in \tilde{\mathbf{G}}$, with $u_i = (\underline{u}_i, \bar{u}_i, \delta_i)$, $i = 1, 2$. Let $Z = Z_V + Z_E$, with Z_V as defined through (8) and Z_E as defined through (10). Then,*

$$k_Z(u_1, u_2) = \boldsymbol{\delta}_1^\top L^+ [(\underline{u}_1, \bar{u}_1), (\underline{u}_2, \bar{u}_2)] \boldsymbol{\delta}_2 + \mathbb{1}_{\text{lf}(e_1)=\text{lf}(e_2)} \sqrt{\ell(e_1)\ell(e_2)} k_T(|t(\underline{u}_1) - t(\underline{u}_2)|) (\min(\delta_1, \delta_2) - \delta_1\delta_2), \quad (11)$$

where $\boldsymbol{\delta}_i := (1 - \delta_i, \delta_i)^\top$, $i = 1, 2$, and $L^+ [(\underline{u}_1, \bar{u}_1), (\underline{u}_2, \bar{u}_2)]$ represents the 2×2 submatrix of L^+ with rows $(\underline{u}_1, \bar{u}_1)$ and columns $(\underline{u}_2, \bar{u}_2)$.

While noting that this construction is completely general, we also point out that Markovianity properties, whenever aimed, can be achieved through a proper choice of the temporal kernel k_T . A reasonable choice for k_T is the correlation function of an autoregressive process of order one, which is given by:

$$k_T(h) = \lambda^{|h|}, \quad h \in \mathbb{Z}, \quad (12)$$

where $\lambda \in (-1, 1)$ is a free parameter and $h \in \mathbb{Z}$ is the lag.

Notice that the special case $\lambda = 0$, for which $k_T(h) = \mathbb{1}_{h=0}$, corresponds to the static resistance metric provided by Anderes et al. [2020].

Figure 3 depicts some realisations for the process Z_E over an edge for different values of the parameter λ . The parameter λ for the edges plays a similar role of the parameter α for the nodes: their are both closely related to the inter-dependency of the process at different times. Indeed, λ measures how much the process Z_E is correlated between two times $t_1, t_2 \in \text{ls}(e)$. Analogously, the value α as weight of the temporal edge $e \in E_T$, is related to the partial correlation of the endpoints of e given everything else. As a consequence, it is natural to choose a high value of λ for high values of α and vice-versa. We notice that it is natural to choose non-negative values for λ , as we usually expect a non-negative correlation between the values of Z_E for close times.

Using equation (7), we get the following expression for the distance between any two points $u_1, u_2 \in \tilde{\mathbf{G}}$.

$$d(u_1, u_2) = k_Z(u_1, u_1) + k_Z(u_2, u_2) - 2k_Z(u_1, u_2). \quad (13)$$

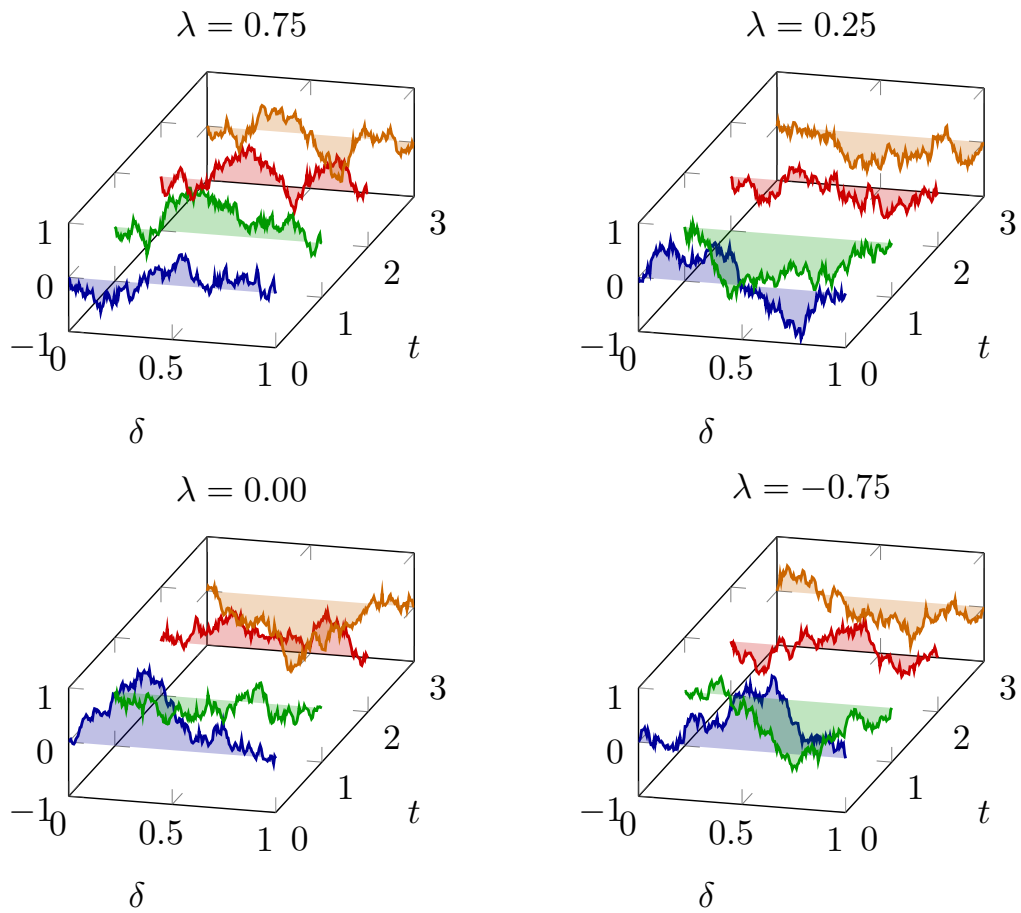


Figure 3: Draws from the process Z_E on an edge with lifespan $\{0, 1, 2, 3\}$, for several values of the parameter λ .

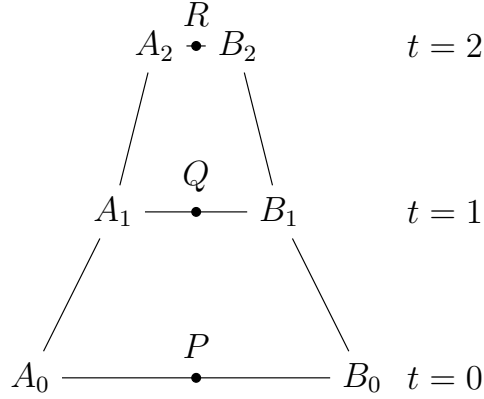


Figure 4: An example of equivalent simple graph for which the semi-distance defined at (13) does not satisfy the triangle inequality.

The formal statement below provides a complete description of the space $(\tilde{\mathbf{G}}, d)$, that is, the time-evolving graph $\tilde{\mathbf{G}}$ equipped with the metric d .

Proposition 2. *Let d be the mapping defined at (13). Then, the pair $(\tilde{\mathbf{G}}, d)$ is a semi-metric space.*

One might ask whether a stronger assertion holds for the pair $(\tilde{\mathbf{G}}, d)$ as defined above. The next statement provides a negative answer.

A counterexample is given by the graph depicted in Figure 4, where the length of the top edge (A_2, B_2) becomes vanishingly small, while length of the bottom edge (A_0, B_0) grows to infinity. For such a graph, we have $d(P, Q) + d(Q, R) < d(P, R)$ (see the proof of Proposition 3 in the Appendix for more details).

Proposition 3. *Let d be the mapping defined at (13). Then, the pair $(\tilde{\mathbf{G}}, d)$ is not a metric space.*

Remark 2. Although in general our extension to the classic resistance distance is not a metric, it retains some of its properties.

1. $(V, d|_V)$ is a metric space.
2. For all t , $(G_t, d|_{G_t})$ coincides with the restriction on G_t of the resistance metric of Anderes et al. [2020] computed on the whole graph $\tilde{\mathbf{G}}$, hence it is a metric and it is invariant to splitting edges and merging edges at degree 2 vertices [Anderes et al., 2020, Propositions 2 and 3].

4.3 A special case: time-evolving linear networks

Anderes et al. [2020] defined graphs with Euclidean edges as a generalisation of linear networks, and Euclidean trees with a given number of leaves. For both cases, edges are linear. This case is not especially exciting for the framework proposed in this paper. The reason is that a simple isometric embedding arguments as in Tang and Zimmerman [2020] proves that one can embed a time-evolving linear network in $\mathbb{R} \times \mathbb{R}^2 = \mathbb{R}^3$, where the first component indicates time. As a consequence, it is immediate to build a vast class of covariance functions on a time-evolving linear network by a sheer restriction of a given covariance function defined on \mathbb{R}^3 . However, such a method does not take into account the *structure* of the graph: two points that are close in \mathbb{R}^3 but far in the time-evolving graph could have a high correlation. Section 6 illustrates how to build kernels over the special topologies proposed in this paper. Apparently, the choices are more restrictive than the ones available for the case of linear networks, but they ensure that the spatio-temporal structure is taken into account.

5 Circular time and periodic graphs

Perhaps the main drawback of using the resistance distance in the layer graphs that express the spatio-temporal variability is that, when adding one or more new layers, the distances between the points of the previous layers may change (more specifically: they may decrease). Indeed, whenever new paths between a couple of points are added, the effective distance between such points decreases, as the current meets less resistance. This presents a critical interpretation problem: for a given time series, let new data be added on a daily basis. Then, inference routines may provide different results when compared to the results of same inference techniques applied to the updated time series. Indeed, as the distances may vary, the covariances between the same space-time points may vary as well.

Here, we consider the alternative of time-evolving *periodic* networks, *i.e.* time-evolving networks whose evolution repeats after a fixed amount of time instants (number of layers). Not only does this construction solve the above-mentioned issue, but it also suits many phenomena whose evolution present both linear and periodic components.

Definition 4 (Time-evolving periodic graph). Let $\mathbf{G} = \{G_0, G_1, \dots\}$ be a

countable sequence of graphs. Then, \mathbf{G} is a *time-evolving periodic graph* if there exists a natural number $m \geq 3$ such that, for all $t \in \mathbb{N}$, $G_t = G_{t+m}$. Its equivalent simple Markovian periodic graph $\tilde{\mathbf{G}}$ is built by connecting G_0, \dots, G_{m-1} through the set of edges

$$E_T = \{(v_1, v_2) \in V \times V : s(v_1) = s(v_2), |t(v_1) - t(v_2)| \equiv \pm 1 \pmod{m}\}. \quad (14)$$

Each point in the resulting space-time is denoted by its true time $t \in \mathbb{R}_0^+$, by the endpoints of the edge e it lies on and by the relative distance $\delta_e(u)$ from the first one: we write $u = (t, \underline{u}, \bar{u}, \delta_e(u))$, where $e = (\underline{u}, \bar{u})$. Notice that $t \in \mathbb{N}$ whenever u belongs to a temporal layer, while t is not integer if u belongs to the inner part of a temporal edge $e \in E_T$. Given a point $u \in V \cup \bigcup E_S$, we sometimes write $\tau(u)$ as the unique layer $\tau \in \{0, \dots, m-1\}$ that contains u . Clearly $\tau(u) \equiv t(u) \pmod{m}$.

We start by noting that the previously-mentioned issue about linear time-evolving graphs is overcome by this construction. Indeed, once the full periodic structure has been established, the Laplacian matrix needs be computed only once, regardless of how many new time points are added.

A second remark comes from the metric construction, which necessarily needs to be adapted to a periodic process. Otherwise, some counter-intuitive properties can arise. Suppose the distance $d(u_1, u_2)$ is defined as in (7). Then, for any couple of points $u_1 = (t_1, \underline{u}_1, \bar{u}_1, \delta_e(u_1))$ and $u_2 = (t_2, \underline{u}_2, \bar{u}_2, \delta_e(u_2))$ with $\underline{u}_1 = \underline{u}_2$, $\bar{u}_1 = \bar{u}_2$ and $\delta_e(u_1) = \delta_e(u_2)$, even when $t_1 \neq t_2$, the distance would be identically equal to zero. Hence, a different definition for the process Z is necessary.

For a point $u = (t, \underline{u}, \bar{u}, \delta_e(u)) \in \tilde{\mathbf{G}}$, we define the process Z for the periodic graph as follows:

$$Z(u) := Z_V(u) + Z_E(u) + \beta W(t), \quad (15)$$

where $\beta > 0$ is a given parameter, W is a standard Wiener process, Z_V is the same process as in the linear-time case, while Z_E , albeit similar, presents some difference with respect to the construction given in Subsection 4.1, aimed to capture the time structure of the periodic graph.

Let $e = (v_1, v_2) \in E_S$: we define the *lifespan* of e as the maximal subset of $\{0, \dots, m-1\}$ such that:

- $\tau(v_1) \in \text{ls}(e)$,

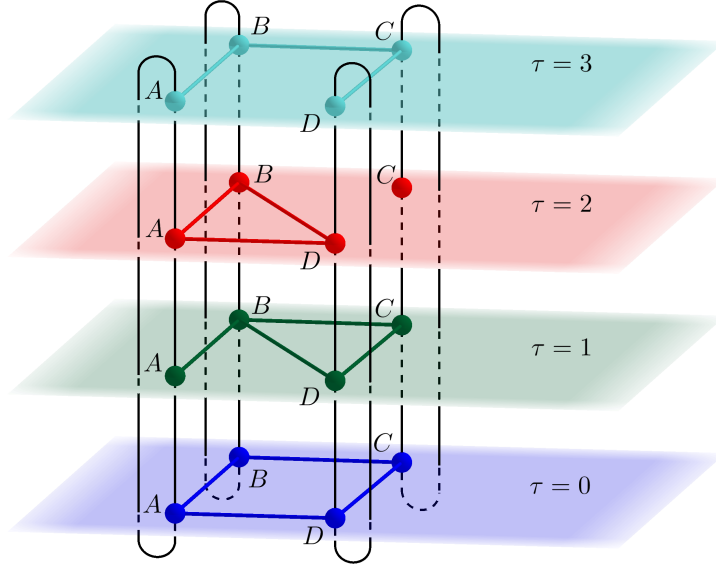


Figure 5: An example of an equivalent simple graph for a periodic time-evolving graph with $m = 4$ and $S = \{A, B, C, D\}$. The coloured edges belong to E_S , whilst the black ones belong to E_T .

- $\text{ls}(e)$ is connected, i.e. if $\tau_1 < \tau_2 \in \text{ls}(e)$, then $\{\tau_1, \dots, \tau_2\} \subseteq \text{ls}(e)$ or $\{\tau_2, \dots, m-1, 0, \dots, \tau_1\} \subseteq \text{ls}(e)$,
- $\forall \tau \in \text{ls}(e), \exists (v'_1, v'_2) \in E_S$ such that $s(v'_1) = s(v_1), s(v'_2) = s(v_2)$ and $\tau(v'_1) = \tau(v'_2) = \tau$.

Figure 5 depicts this situation. Here, the lifespan of the edge (A, B) at time $\tau = 0$ is $\{0, 1, 2, 3\}$; the lifespan of (A, D) at time $\tau = 2$ is $\{2\}$; the lifespan of (C, D) at time $\tau = 3$ is $\{0, 1, 3\}$.

The definition of life of any edge $e \in E$ remains unchanged: if $e \in E_S$,

$$\text{lf}(e) := \{(v'_1, v'_2) \in E_S : s(v'_1) = s(v_1), s(v'_2) = s(v_2), \tau(v'_1) = \tau(v'_2) \in \text{ls}(e)\}$$

while, if $e \in E_T$, $\text{lf}(e) := \{e\}$.

The definition of Z_E is now identical to the one of the linear-time graph, exception made for the choice of the temporal kernel k_T . Indeed, we ought to consider that the time is now cyclic in the dependence structure of the temporal layers $\tau \in \{0, \dots, m-1\}$. It is reasonable to model the process underlying the temporal kernel k_T by means of a graphical model, as it

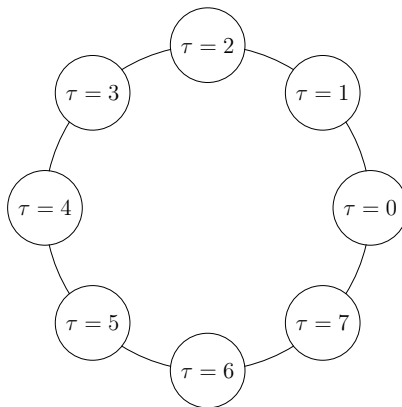


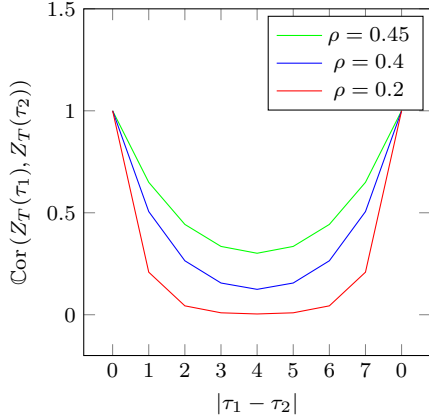
Figure 6: Conditional dependence structure of the process Z_T for $m = 8$.

embodies the idea of conditional independence. For a given spatial edge $e \in E_S$, we distinguish two cases: whether the lifespan of e is the whole temporal set $T = \{0, \dots, m - 1\}$ or not.

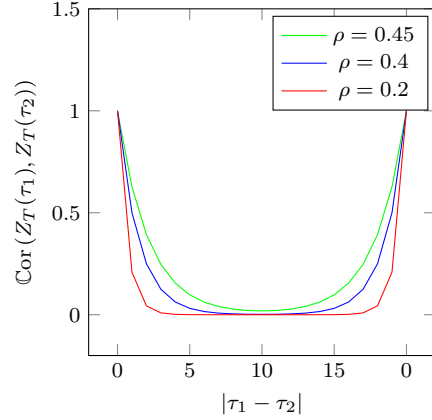
5.1 The lifespan coincides with T

In this case, we define the covariance matrix of a zero-mean Gaussian random vector $Z_T : \{0, \dots, m - 1\} \rightarrow \mathbb{R}$ via its precision matrix. More precisely, let G_T be the circulant graph with m nodes (labelled by $\tau \in \{0, \dots, m - 1\}$) and m edges between adjacent nodes, as shown in Figure 6. We associate each edge with a given weight $\rho \in [0, \frac{1}{2})$, which represents the partial correlation between subsequent times. As a consequence, the precision matrix Θ_{Z_T} is the circulant matrix that follows.

$$\Theta_{Z_T} = \kappa \begin{bmatrix} 1 & -\rho & 0 & \dots & 0 & -\rho \\ -\rho & 1 & -\rho & \dots & 0 & 0 \\ 0 & -\rho & 1 & \dots & 0 & 0 \\ \vdots & \vdots & \vdots & \ddots & \vdots & \vdots \\ 0 & 0 & 0 & \dots & 1 & -\rho \\ -\rho & 0 & 0 & \dots & -\rho & 1 \end{bmatrix}$$



The correlations of Z_T for some values of ρ and $m = 8$.



The correlations of Z_T for some values of ρ and $m = 20$.

Figure 7: Some examples of the correlation functions k_T in the case $\text{ls}(e) = \{0, \dots, m-1\}$.

Here, $\kappa > 0$ is a normalising constant which role is to make the covariance matrix $\Sigma_{Z_T} := (\Theta_{Z_T})^{-1}$ a correlation matrix (namely the variances of every entry of Z_T should be 1). Notice that the matrix Σ_{Z_T} is a symmetric circulant matrix: as a consequence, it is possible to store only its first column, which will be denoted by $\sigma_{Z_T} \in \mathbb{R}^m$. In Figure 7, the values of the vector σ_{Z_T} are plotted for some values of m and ρ .

5.2 The lifespan does not coincide with T

In this case, the life of the edge e is interrupted. Thus, it is reasonable to consider the different parts of the life of e as independent. To this aim, we consider the subgraph of G_T that represents the evolution of the edge e . More precisely, we remove from G_T all the nodes τ for which the edge e does not exist and we remove from G_T all the edges whose at least one endpoint has been eliminated. Next, we consider all the connected components of the so-obtained graph and define an autoregressive model on each of them, independently from the others (similarly to the linear case of Section 4.2). More precisely, we define the covariance matrix of the process Z_T as a block-

diagonal matrix whose diagonal blocks are of the form

$$\begin{bmatrix} 1 & \lambda & \dots & \lambda^{j-1} \\ \lambda & 1 & \dots & \lambda^{j-2} \\ \vdots & \vdots & \ddots & \vdots \\ \lambda^{j-1} & \lambda^{j-2} & \dots & 1 \end{bmatrix},$$

being $\lambda \in (-1, 1)$ the lag-1 correlation and j the number of times τ that belong to $\text{ls}(e)$, *i.e.* $j := |\text{ls}(e)|$.

5.3 Second-order properties of Z in the circular case

The following result illustrates the analytic expression for the covariance function associated with Z in the construction of the metric associated with $\tilde{\mathbf{G}}$ in the periodic case.

Proposition 4. *Let $u_1 = (t_1, \underline{u}_1, \bar{u}_1, \delta_e(u_1)) \in \tilde{\mathbf{G}}$ and $u_2 = (t_2, \underline{u}_2, \bar{u}_2, \delta_e(u_2)) \in \tilde{\mathbf{G}}$. Then the kernel of the process Z defined on $\tilde{\mathbf{G}}$ enjoys the following representation:*

$$\begin{aligned} k_Z(u_1, u_2) &= \boldsymbol{\delta}_1^\top L^+ [(\underline{u}_1, \bar{u}_1), (\underline{u}_2, \bar{u}_2)] \boldsymbol{\delta}_2 \\ &\quad + \mathbb{1}_{\text{lf}(e_1)=\text{lf}(e_2)} \sqrt{\ell(e_1)\ell(e_2)} k_T(\tau(\underline{u}_1), \tau(\underline{u}_2)) (\min(\delta_1, \delta_2) - \delta_1\delta_2) \\ &\quad + \beta^2 \min(t_1, t_2) \end{aligned} \tag{16}$$

where $\boldsymbol{\delta}_i := (1 - \delta_i, \delta_i)^\top$ and $L^+ [(\underline{u}_1, \bar{u}_1), (\underline{u}_2, \bar{u}_2)]$ represents the 2×2 sub-matrix of L^+ with rows $(\underline{u}_1, \bar{u}_1)$ and columns $(\underline{u}_2, \bar{u}_2)$.

Notice that the unique differences with the expression (11) are the different choices for the temporal kernel k_T and the additional addend $\beta^2 \min(t_1, t_2)$. The latter ensures that the same points at different times have a strictly positive distance, as, combining equations (13) and (16) for such points u_1 and u_2 , we get $d(u_1, u_2) = \beta^2 |t_1 - t_2|$.

We conclude this section with a formal assertion regarding the mapping d as being introduced for the case of a periodic graph \mathbf{G} .

Proposition 5. *$(\tilde{\mathbf{G}}, d)$ is a semi-metric space.*

Type	$\psi(x)$	Parameter range
Power exponential	$e^{-\beta x^\alpha}$	$0 < \alpha \leq 1, \beta > 0$
Matérn	$\frac{2^{1-\alpha}}{\Gamma(\alpha)} (\beta x)^\alpha K_\alpha(\beta x)$	$0 < \alpha \leq \frac{1}{2}, \beta > 0$
Generalised Cauchy	$(\beta x^\alpha + 1)^{-\xi/\alpha}$	$0 < \alpha \leq 1, \beta > 0, \xi > 0$
Dagum	$1 - \left(\frac{\beta x^\alpha}{1 + \beta x^\alpha} \right)^{\xi/\alpha}$	$0 < \alpha \leq 1, 0 < \xi \leq 1, \beta > 0$

Table 1: Examples of completely monotone functions $0 \leq x \mapsto \psi(x)$ such that $\psi(0) = 1$. Here, K_r denotes the modified Bessel function of the second kind.

6 Reproducing kernels

6.1 General construction principles

Variograms can be composed with certain classes of functions to create reproducing kernels associated with semi-metric spaces. A function $\psi : [0, +\infty) \rightarrow \mathbb{R}$ is called *completely monotone* if it is continuous on $[0, +\infty)$, infinitely differentiable on $(0, +\infty)$ and for each $i \in \mathbb{N}$ it holds

$$(-1)^i \psi^{(i)}(x) \geq 0,$$

where $\psi^{(i)}$ denotes the i^{th} derivative of ψ and $\psi^{(0)} := \psi$. By the celebrated Bernstein's theorem [Bernstein, 1929], completely monotone functions are the Laplace transforms of positive and bounded measures. Some examples of parametric families of completely monotone functions are listed in Table 1.

The result below comes straight by using similar arguments as in Anderes et al. [2020], which have been reported in Theorem 1 in Appendix B.

Proposition 6. *Let $\psi : [0, \infty) \rightarrow \mathbb{R}$ be continuous, completely monotonic on the positive real line, and with $\psi(0) < \infty$. Let $d : \tilde{\mathbf{G}} \times \tilde{\mathbf{G}} \rightarrow \mathbb{R}$ be the mapping defined at (13). Then, the function*

$$k_Z(u_1, u_2) = \psi(d(u_1, u_2)), \quad u_1, u_2 \in \tilde{\mathbf{G}}$$

is a strictly positive definite function.

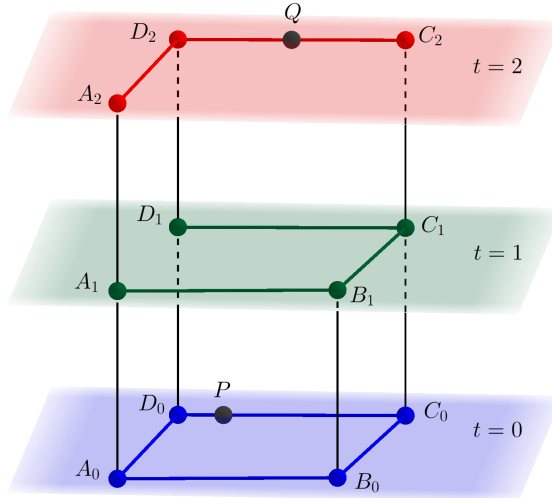


Figure 8: Equivalent simple graph taken as an example for the linear-time case.

Proposition 6 provides a very easy recipe to build kernels over time evolving graphs, whatever the temporal structure (linear or periodic). Any element from the Table 1 is a good candidate for such a composition. We do not report the corresponding algebraic forms for obvious reasons. Instead, we concentrate on illustrating how these covariance works through two practical examples. We believe that the free parameters and the large number of analytically-tractable completely monotone functions provide a wide range of models that could fit several real-world frameworks.

6.2 Linear time

We start by considering the graph in Figure 8. Here, we have $m = 3$ time instants. Further,

$$V = \{A_0, B_0, C_0, D_0, A_1, B_1, C_1, D_1, A_2, C_2, D_2\}.$$

We focus on the distances as well as the covariances between the points $A_0 = (A_0, B_0, \delta_{A_0} = 0)$, $P := (C_0, D_0, \delta_P = 0.8)$ and $Q := (C_2, D_2, \delta_Q = 0.5)$. All the spatial edges E_S have weight 1, whilst the temporal edges have weight

$\alpha > 0$. Finally, we use k_T as in (12), with λ free parameter. The adjacency matrix follows (here \cdot stands for 0).

$$\begin{bmatrix} \cdot & 1 & \cdot & 1 & \alpha & \cdot & \cdot & \cdot & \cdot & \cdot & \cdot \\ 1 & \cdot & 1 & \cdot & \cdot & \alpha & \cdot & \cdot & \cdot & \cdot & \cdot \\ \cdot & 1 & \cdot & 1 & \cdot & \cdot & \alpha & \cdot & \cdot & \cdot & \cdot \\ 1 & \cdot & 1 & \cdot & \cdot & \cdot & \cdot & \alpha & \cdot & \cdot & \cdot \\ \alpha & \cdot & \cdot & \cdot & \cdot & 1 & \cdot & \cdot & \alpha & \cdot & \cdot \\ \cdot & \alpha & \cdot & \cdot & 1 & \cdot & 1 & \cdot & \cdot & \cdot & \cdot \\ \cdot & \cdot & \alpha & \cdot & \cdot & 1 & \cdot & 1 & \cdot & \alpha & \cdot \\ \cdot & \cdot & \cdot & \alpha & \cdot & \cdot & 1 & \cdot & \cdot & \cdot & \alpha \\ \cdot & \cdot & \cdot & \cdot & \alpha & \cdot & \cdot & \cdot & \cdot & \cdot & 1 \\ \cdot & \cdot & \cdot & \cdot & \cdot & \cdot & \alpha & \cdot & \cdot & \cdot & 1 \\ \cdot & \cdot & \cdot & \cdot & \cdot & \cdot & \cdot & \alpha & 1 & 1 & \cdot \end{bmatrix}$$

Figure 9 clearly shows the effect the temporal edge parameter α plays on the distances: while it has a considerable impact on the distances $d(A_0, Q)$ and $d(P, Q)$, it shows a negligible effect on $d(A_0, P)$. This is reasonable given the graph structure: A_0 and P belong to the same layer ($t = 0$) and they are connected from both the paths A_0, D_0, P and A_0, B_0, C_0, P , which completely lie on $t = 0$ (and therefore they do not change with α). On the other hand, Q can be connected to A_0 and P only via paths that include temporal edges. As a consequence, if $\alpha \rightarrow 0^+$, both $d(A_0, Q)$ and $d(P, Q)$ will go to infinity.

The plot on the right of Figure 9 shows the effect of the correlation parameter λ as well. Whilst it does not influence the distances concerning A_0 (since it is a vertex), as it increase, it reduces the distances between P and Q . Clearly, the effect is more significant for large values of the parameter α . Indeed, when α is small, the distances between nodes at different time instants are large. As a consequence, the second line of equation (11) becomes negligible when compared to the first one.

Figure 10 shows the resulting effect of the parameter α on the correlations between A_0, P and Q generated by the composition of two completely monotone functions taken from Table 1 and the distances shown in Figure 9.

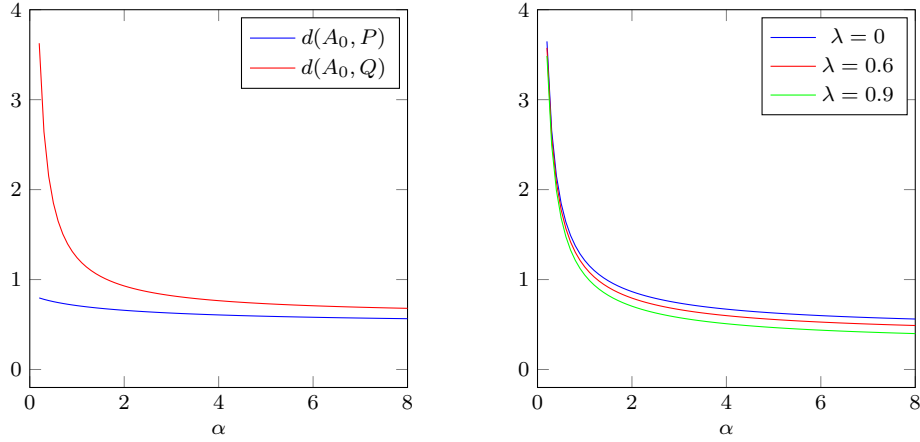


Figure 9: Distances between the points A_0 , P and Q . Notice that while $d(A_0, P)$ and $d(A_0, Q)$ (left) do not depend on λ , the distance $d(P, Q)$ (right) decreases as λ increases.

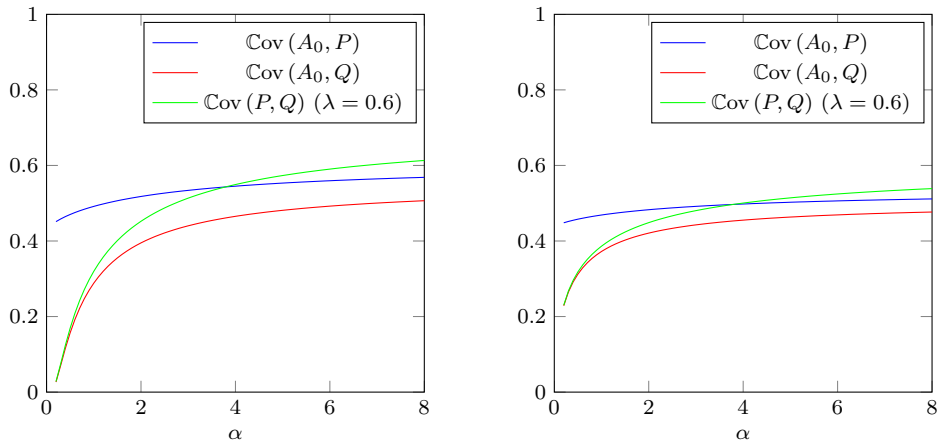


Figure 10: Generated covariances between the points A_0 , P and Q . Left: exponential kernel with parameters $(\alpha = 1, \beta = 1)$ (see Table 1). Right: generalised Cauchy kernel with parameters $(\alpha = 1, \beta = 5, \xi = 0.5)$ (see Table 1).

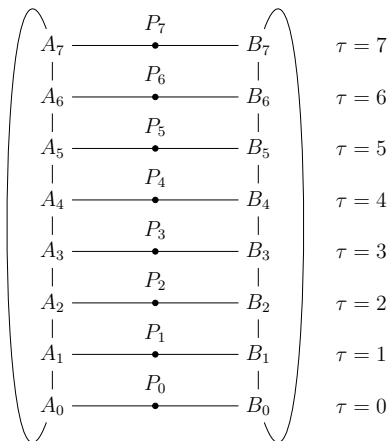


Figure 11: Equivalent simple graph taken as an example for the circular-time case.

6.3 Circular time

We are going to analyse the time-evolving periodic graph depicted in Figure 11. In this case, we have $m = 8$ and

$$V = \{A_0, B_0, A_1, B_1, \dots, A_7, B_7\}.$$

We will compare the distances and the covariances between the points $P_0 := (0, A_0, B_0, \delta_{P_0} = 0.5)$ and $P_t := (t, A_\tau, B_\tau, \delta_{P_t} = 0.5)$, where $t \in \mathbb{N}$ and $\tau \equiv t \pmod{m}$. Here, all the spatial edges have weight 1, whilst the temporal ones have weight $\alpha > 0$. We use the temporal kernel k_T as described in Subsection 5.1, with ρ and β free parameters.

The distances and covariances in Figure 12 show the effect of the parameter β on our construction. It adds a linear component $\beta^2 t$, which allows to calibrate the distance (and, as a result, the covariance) between the points at different time instants. In such a way, the effect of the periodicity is increased by setting a low β and becomes negligible when β grows. Furthermore, notice

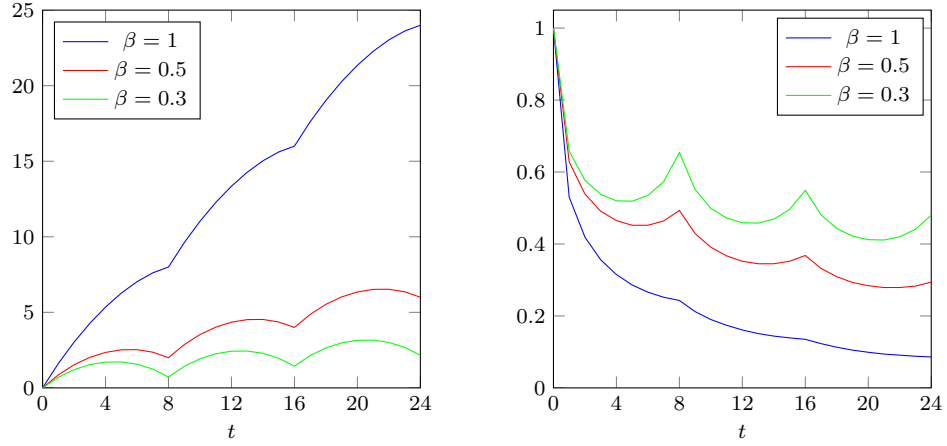


Figure 12: Distances (left) and covariances (right) for the graph in Figure 11 between the points P_0 and P_t for $\rho = 0.45$ and $\alpha = 1$. Covariances have been generated via the exponential kernel with parameters $\alpha = 0.5$ and $\beta = 0.5$ (see Table 1).

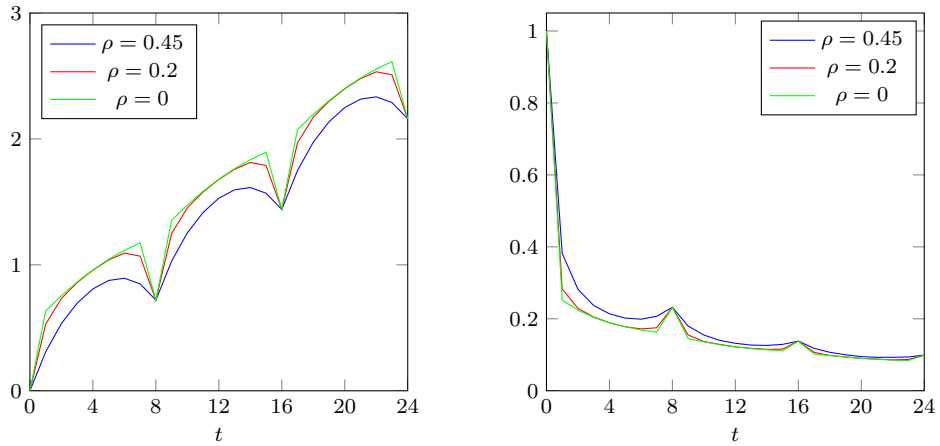


Figure 13: Distances (left) and covariances (right) for the graph in Figure 11 between the points P_0 and P_t for $\alpha = 10$ and $\beta = 0.3$. Covariances have been generated via the Dagum kernel with parameters $\alpha = 1$, $\beta = 2$ and $\xi = 0.5$ (see Table 1).

the spikes the covariance functions show: they perfectly embody the periodic setting of a process, as introduced in Subsection 1.3. It is in order to remark that, although isotropic covariances are decreasing functions of the spatial distances, Figures 12 and 13 show valid covariance functions, as the distance of our setting is completely different from the Euclidean distance on \mathbb{R}^n as it takes into account the spatio-temporal structure of the time-evolving graph.

In Figure 13, it is possible to visualise the effect of the partial correlation parameter $\rho \in [0, \frac{1}{2})$. First, notice that its role is particularly significant when the weight α is high. Indeed, for low α 's, the covariance structure of the vertices given by the inverse laplacian matrix is dominant. Yet, when α is high, the nodes at different time instants are considered close to each other and the resulting distances given by the sheer first line of (16) are low. Thus, the parameter ρ (which enters in the second line of (16)) has a greater influence. Clearly, the greater is ρ , the lower is the distance, as it correlates different Brownian bridge realisations.

7 Conclusion: impact of this research

The research presented in this paper provides the fundamentals to a part of literature that had considered networks evolution to a very limited extent. The impact of this research is multifarious:

1. temporal evolution of networks is preoccupying many scientists in both theoretical and applied disciplines. In network design problems (NDP), the optimal selection of subgraphs is a major issue. Several applications of generalised NDP arise in the fields of telecommunications, transportation and biology, and the reader is referred to [Feremans et al. \[2003\]](#), with the references therein. Dealing with these kind of problems under the framework presented here will be a major task.
2. Most of the approaches about generalised networks are computer based, and the attention has been largely put on algorithmic complexity rather than on mathematical and statistical accuracy, see [Harrington and Mautz \[1976\]](#) and [Glover et al. \[1978\]](#), for instance. Here, we have provided an analytic effort, and the computational burden has been taken care thanks to the assumption of temporal Markovianity.
3. Several emerging fields are increasingly working over generalised networks. Yet, temporal evolution has been considered under overly re-

strictive assumptions. Crime data on networks have been considered with strong emphasis on computer and algorithmic complexity [Chen et al., 2004]. More recently there has been a considerable interest in the statistical assessment of such data over networks, and the reader is referred to Bernasco and Elffers [2010], and the more recent paper by Firinguetti et al. [2023], with the references therein. The connections (correlations and causalities) studied through generalised networks are of main interests in psychometrics [Epskamp et al., 2017] and in genetics [Yip and Horvath, 2007], and the literature is starting to produce contributions where the interconnections are continuously defined over the edges and not only at the nodes.

Several fundamental research questions are then inspired on the contribution in this paper. To mention a few, regularity properties of temporally evolving stochastic processes defined over generalised networks can now be studied thanks to the framework provided in this paper. Another field of research that will benefit from our research is that of stream flows, where the graphs are oriented (think about a river with currents in a given direction). In finance, there is a fertile literature on causality, with special emphasis on graph causality, and the reader is referred to the monumental effort in Lopez de Prado [2022]. Studying causality under continuity—as in our approach—is definitely a major challenge for the future.

Other major theoretical challenges involve the definition of multivariate processes over generalised networks. Further, it is imperative to relax the assumptions of stationarity and isotropy. All these will be major challenges for future researches.

Acknowledgements

The authors are grateful to Havard Rue for insightful discussions during the preparation of this manuscript. This project has also been sustained by the prompt help of Valeria Simoncini.

References

Sameer Agarwal, Kristin Branson, and Serge Belongie. Higher order learning with graphs. In *Proceedings of the 23rd international conference on*

- Machine learning*, pages 17–24, 2006.
- Mohammad Abu Alsheikh, Shaowei Lin, Dusit Niyato, and Hwee-Pink Tan. Machine learning in wireless sensor networks: Algorithms, strategies, and applications. *IEEE Communications Surveys & Tutorials*, 16(4):1996–2018, 2014.
- Ethan Anderes, Jesper Møller, and Jakob G Rasmussen. Isotropic covariance functions on graphs and their edges. *Annals of Statistics*, 48(4):2478–2503, 2020.
- Adrian Baddeley, Gopalan Nair, Suman Rakshit, and Greg McSwiggan. Stationary point processes are uncommon on linear networks. *Stat*, 6(1):68–78, 2017.
- Adrian Baddeley, Gopalan Nair, Suman Rakshit, Greg McSwiggan, and Tilman M. Davies. Analysing point patterns on networks – a review. *Spatial Statistics*, 42:100435, 2021. ISSN 2211-6753. doi: <https://doi.org/10.1016/j.spasta.2020.100435>. URL <https://www.sciencedirect.com/science/article/pii/S2211675320300294>. Towards Spatial Data Science.
- Wim Bernasco and Henk Elffers. Statistical analysis of spatial crime data. *Handbook of quantitative criminology*, pages 699–724, 2010.
- Serge Bernstein. Sur les fonctions absolument monotones. *Acta Mathematica*, 52:1–66, 1929. ISSN 0001-5962, 1871-2509. doi: 10.1007/BF02592679. URL <https://projecteuclid.org/journals/acta-mathematica/volume-52/issue-none/Sur-les-fonctions-absolument-monotones/10.1007/BF02592679.full>. Publisher: Institut Mittag-Leffler.
- D. Bolin and F. Lindgren. Spatial Models Generated by Nested Stochastic Partial Differential Equations, with an Application to Global Ozone Mapping. *Ann. Appl. Statist.*, 5(1):523–550, 2011.
- David Bolin, Alexandre B Simas, and Jonas Wallin. Gaussian Whittle-Matérn fields on metric graphs. *arXiv preprint arXiv:2205.06163*, 2022.
- Viacheslav Borovitskiy, Iskander Azangulov, Alexander Terenin, Peter Mostowsky, Marc Deisenroth, and Nicolas Durrande. Matérn gaussian

- processes on graphs. In Arindam Banerjee and Kenji Fukumizu, editors, *Proceedings of The 24th International Conference on Artificial Intelligence and Statistics*, volume 130 of *Proceedings of Machine Learning Research*, pages 2593–2601. PMLR, 13–15 Apr 2021. URL <https://proceedings.mlr.press/v130/borovitskiy21a.html>.
- Viacheslav Borovitskiy, Mohammad Reza Karimi, Vignesh Ram Somnath, and Andreas Krause. Isotropic gaussian processes on finite spaces of graphs. *arXiv preprint arXiv:2211.01689*, 2022.
- Viacheslav Borovitskiy, Mohammad Reza Karimi, Vignesh Ram Somnath, and Andreas Krause. Isotropic gaussian processes on finite spaces of graphs. In Francisco Ruiz, Jennifer Dy, and Jan-Willem van de Meent, editors, *Proceedings of The 26th International Conference on Artificial Intelligence and Statistics*, volume 206 of *Proceedings of Machine Learning Research*, pages 4556–4574. PMLR, 25–27 Apr 2023. URL <https://proceedings.mlr.press/v206/borovitskiy23a.html>.
- Ines Chami, Sami Abu-El-Haija, Bryan Perozzi, Christopher Ré, and Kevin Murphy. Machine learning on graphs: A model and comprehensive taxonomy. *The Journal of Machine Learning Research*, 23(1):3840–3903, 2022.
- Hsinchun Chen, Wingyan Chung, Jennifer Jie Xu, Gang Wang, Yi Qin, and Michael Chau. Crime data mining: a general framework and some examples. *Computer*, 37(4):50–56, 2004.
- Hocine Cherifi, Gergely Palla, Boleslaw Szymanski, and Xiaoyan Lu. On community structure in complex networks: challenges and opportunities. *Applied Network Science*, 4, 12 2019. doi: 10.1007/s41109-019-0238-9.
- Noel Cressie, Jesse Frey, Bronwyn Harch, and Mick Smith. Spatial prediction on a river network. *Journal of Agricultural, Biological, and Environmental Statistics*, 11(2):127, 2006.
- Na Deng, Wuyang Zhou, and Martin Haenggi. The ginibre point process as a model for wireless networks with repulsion. *IEEE Transactions on Wireless Communications*, 14(1):107–121, 2014.
- Karel Devriendt. Effective resistance is more than distance: Laplacians, simplices and the Schur complement. *Linear Algebra and its Applications*,

- 639:24–49, 2022. ISSN 00243795. doi: 10.1016/j.laa.2022.01.002. URL <http://arxiv.org/abs/2010.04521>.
- Aswathy Divakaran and Anuraj Mohan. Temporal link prediction: A survey. *New Generation Computing*, 38(1):213–258, 2020. ISSN 0288-3635, 1882-7055. doi: 10.1007/s00354-019-00065-z. URL <http://link.springer.com/10.1007/s00354-019-00065-z>.
- Sacha Epskamp, Mijke Rhemtulla, and Denny Borsboom. Generalized network psychometrics: Combining network and latent variable models. *Psychometrika*, 82:904–927, 2017.
- Corinne Feremans, Martine Labbé, and Gilbert Laporte. Generalized network design problems. *European Journal of Operational Research*, 148(1): 1–13, 2003.
- L. Firinguetti, T. Faouzi, L. Lara Carrión, G. Muschert, and E. Porcu. Understanding the space-time distribution of robberies: The case of san pedro de la paz, chile. *Technical Report, Khalifa University. Submitted for Publication to Crime Science*, 2023.
- Beth Gardner, Patrick J Sullivan, and Arthur J Lembo, Jr. Predicting stream temperatures: geostatistical model comparison using alternative distance metrics. *Canadian Journal of Fisheries and Aquatic Sciences*, 60(3):344–351, 2003.
- Leonidas Georgopoulos and Martin Hasler. Distributed machine learning in networks by consensus. *Neurocomputing*, 124:2–12, 2014.
- Arpita Ghosh, Stephen Boyd, and Amin Saberi. Minimizing effective resistance of a graph. *SIAM Review*, 50(1):37–66, 2008. ISSN 0036-1445. doi: 10.1137/050645452. URL <https://epubs.siam.org/doi/10.1137/050645452>. Publisher: Society for Industrial and Applied Mathematics.
- Fred Glover, John Hultz, Darwin Klingman, and J Stutz. Generalized networks: A fundamental computer-based planning tool. *Management Science*, 24(12):1209–1220, 1978.
- William L Hamilton, Rex Ying, and Jure Leskovec. Representation learning on graphs: Methods and applications. *arXiv preprint arXiv:1709.05584*, 2017.

- Steve Hanneke, Wenjie Fu, and Eric P. Xing. Discrete temporal models of social networks. *Electronic Journal of Statistics*, 4:585 – 605, 2010. doi: 10.1214/09-EJS548. URL <https://doi.org/10.1214/09-EJS548>.
- R Harrington and J Mautz. A generalized network formulation for aperture problems. *IEEE Transactions on Antennas and Propagation*, 24(6):870–873, 1976.
- Thomas Hofmann, Bernhard Schölkopf, and Alexander J Smola. A review of kernel methods in machine learning. *Mac-Planck-Institute Technical Report*, 156, 2006.
- Thomas Hofmann, Bernhard Schölkopf, and Alexander J. Smola. Kernel methods in machine learning. *The Annals of Statistics*, 36(3):1171 – 1220, 2008. doi: 10.1214/009053607000000677. URL <https://doi.org/10.1214/009053607000000677>.
- Weihua Hu, Matthias Fey, Marinka Zitnik, Yuxiao Dong, Hongyu Ren, Bowen Liu, Michele Catasta, and Jure Leskovec. Open graph benchmark: Datasets for machine learning on graphs. *Advances in neural information processing systems*, 33:22118–22133, 2020.
- Weihua Hu, Matthias Fey, Hongyu Ren, Maho Nakata, Yuxiao Dong, and Jure Leskovec. Ogb-lsc: A large-scale challenge for machine learning on graphs. *arXiv preprint arXiv:2103.09430*, 2021.
- Palle E. T. Jorgensen and Erin Peter James Pearse. A Hilbert space approach to effective resistance metric. *Complex Analysis and Operator Theory*, 4(4): 975–1013, 2010. ISSN 1661-8262. doi: 10.1007/s11785-009-0041-1. URL <https://doi.org/10.1007/s11785-009-0041-1>.
- Sun Yuan Kung. *Kernel methods and machine learning*. Cambridge University Press, 2014.
- Steffen L Lauritzen. *Graphical models*, volume 17. Clarendon Press, 1996.
- Marcus Lim, Azween Abdullah, Noor Jhanjhi, and Khurram Khan. Link prediction in time-evolving criminal network with deep reinforcement learning technique. *IEEE Access*, PP:1–1, 2019. doi: 10.1109/ACCESS.2019.2958873.

- Marcos Lopez de Prado. Causal factor investing: Can factor investing become scientific? *Available at SSRN 4205613*, 2022.
- Shawn Mankad and George Michailidis. Structural and functional discovery in dynamic networks with non-negative matrix factorization. *Physical Review. E, Statistical, Nonlinear, and Soft Matter Physics*, 88(4):042812, 2013. ISSN 1550-2376. doi: 10.1103/PhysRevE.88.042812.
- Valdir Menegatto, Claudemir Oliveira, and Emilio Porcu. Gneiting class, semi-metric spaces and isometric embeddings. *Constructive Mathematical Analysis*, 3(2):85–95, 2020.
- Maxime Montembeault, Sven Joubert, Julien Doyon, Julie Carrier, Jean-François Gagnon, Oury Monchi, Ovidiu Lungu, Sylvie Belleville, and Simona Maria Brambati. The impact of aging on gray matter structural covariance networks. *Neuroimage*, 63(2):754–759, 2012.
- M.M. Moradi and J. Mateu. First-and second-order characteristics of spatio-temporal point processes on linear networks. *Journal of Computational and Graphical Statistics*, 29(3):432–443, 2020.
- Maximilian Nickel, Kevin Murphy, Volker Tresp, and Evgeniy Gabrilovich. A review of relational machine learning for knowledge graphs. *Proceedings of the IEEE*, 104(1):11–33, 2015.
- Patrick O Perry and Patrick J Wolfe. Point process modelling for directed interaction networks. *Journal of the Royal Statistical Society: Series B*, 75(5):821–849, 2013.
- Erin E Peterson, David M Theobald, and Jay M ver Hoef. Geostatistical modelling on stream networks: developing valid covariance matrices based on hydrologic distance and stream flow. *Freshwater Biology*, 52(2):267–279, 2007.
- Erin E Peterson, Jay M Ver Hoef, Dan J Isaak, Jeffrey A Falke, Marie-Josée Fortin, Chris E Jordan, Kristina McNyset, Pascal Monestiez, Aaron S Ruesch, Aritra Sengupta, et al. Modelling dendritic ecological networks in space: an integrated network perspective. *Ecology Letters*, 16(5):707–719, 2013.

- Gianluigi Pillonetto, Francesco Dinuzzo, Tianshi Chen, Giuseppe De Nicolao, and Lennart Ljung. Kernel methods in system identification, machine learning and function estimation: A survey. *Automatica*, 50(3):657–682, 2014.
- Thomas Pinder, Kathryn Turnbull, Christopher Nemeth, and David Leslie. Gaussian processes on hypergraphs. *arXiv preprint arXiv:2106.01982*, 2021.
- Emilio Porcu, Moreno Bevilacqua, and Marc G. Genton. Spatio-temporal covariance and cross-covariance functions of the great circle distance on a sphere. *Journal of the American Statistical Association*, 111(514):888–898, 2016. doi: 10.1080/01621459.2015.1072541. URL <http://dx.doi.org/10.1080/01621459.2015.1072541>.
- Emilio Porcu, Moreno Bevilacqua, Robert Schaback, and Chris J Oates. The matérn model: A journey through statistics, numerical analysis and machine learning. *arXiv preprint arXiv:2303.02759*, 2023a.
- Emilio Porcu, Philip A White, and Marc G Genton. Stationary nonseparable space-time covariance functions on networks. *Journal of the Royal Statistical Society Series B: Statistical Methodology*, page qkad082, 09 2023b. ISSN 1369-7412. doi: 10.1093/jrsss/qkad082. URL <https://doi.org/10.1093/jrsss/qkad082>.
- Suman Rakshit, Gopalan Nair, and Adrian Baddeley. Second-order analysis of point patterns on a network using any distance metric. *Spatial Statistics*, 22:129–154, 2017.
- Ryan A. Rossi, Brian Gallagher, Jennifer Neville, and Keith Henderson. Modeling dynamic behavior in large evolving graphs. In *Proceedings of the sixth ACM international conference on Web search and data mining*, pages 667–676. ACM, 2013. ISBN 978-1-4503-1869-3. doi: 10.1145/2433396.2433479. URL <https://dl.acm.org/doi/10.1145/2433396.2433479>.
- I. J. Schoenberg. Positive Definite Functions on Spheres. *Duke Math. Journal*, 9:96–108, 1942.
- Ljubiša Stanković, Danilo Mandić, Miloš Daković, Miloš Brajović, Bruno Scalzo, Shengxi Li, Anthony G Constantinides, et al. Data analytics on

- graphs part iii: Machine learning on graphs, from graph topology to applications. *Foundations and Trends® in Machine Learning*, 13(4):332–530, 2020.
- M. L. Stein. *Statistical Interpolation of Spatial Data: Some Theory for Kriging*. Springer, New York, 1999.
- Jun Tang and Dale Zimmerman. Space-time covariance models on networks with an application on streams. *arXiv:2009.14745*, 2020.
- Jay M Ver Hoef, Erin Peterson, and David Theobald. Spatial statistical models that use flow and stream distance. *Environmental and Ecological Statistics*, 13(4):449–464, 2006.
- Shuai Xiao, Junchi Yan, Xiaokang Yang, Hongyuan Zha, and Stephen Chu. Modeling the intensity function of point process via recurrent neural networks. In *Proceedings of the AAAI Conference on Artificial Intelligence*, volume 31, 2017.
- Andy M Yip and Steve Horvath. Gene network interconnectedness and the generalized topological overlap measure. *BMC bioinformatics*, 8:1–14, 2007.
- Ziwei Zhang, Xin Wang, and Wenwu Zhu. Automated machine learning on graphs: A survey. *arXiv preprint arXiv:2103.00742*, 2021.

A Mathematical background

The material throughout is standard and there are many classical references at hand. We mention [Lauritzen \[1996\]](#) amongst others.

Definition 5 (Simple, connected graph). Let V a finite set (called *vertices* or *nodes*) and let $E \subseteq V \times V$ a set of connections (called *edges*). Then the pair $G := (V, E)$ is called a *graph* or a *network*. We said that a graph G is *simple* if it is *undirected* (videlicet, whenever $(v_1, v_2) \in E$, then necessarily $(v_2, v_1) \in E$) and if it has no self-loops (namely, for all $v \in V$, $(v, v) \notin E$). For an undirected graph G , two nodes $v_1, v_2 \in V$ are *adjacent* if $(v_1, v_2) \in E$. We write $v_1 \sim v_2$ if v_1 and v_2 are adjacent, $v_1 \not\sim v_2$ if they are not.

A *path* between two nodes $v \neq w \in V$ is a finite sequence of vertices $(v = v_1, v_2, \dots, v_p = w)$ such that, $\forall i \in \{1, \dots, p-1\}$, $(v_i, v_{i+1}) \in E$. A *connected component* of a graph G is a maximal subset of vertices $V' \subseteq V$ such that, for each pair of nodes $v, w \in V'$, there is a path between v and w . A graph G is *connected* if there is only one connected component, namely if there is a path between each pair of nodes.

Definition 6 (Moore-Penrose generalised inverse). Let $M \in \mathbb{R}^{n \times n}$ a matrix. Then its *Moore-Penrose generalised inverse* is the unique matrix $M^+ \in \mathbb{R}^{n \times n}$ such that:

- $MM^+M = M$ and $M^+MM^+ = M^+$,
- $MM^+ = (MM^+)^{\top}$ and $M^+M = (M^+M)^{\top}$.

Definition 7 (g -embedding, isometric embedding). Let (X, d) be a semi-metric space and $g : D_X^d \rightarrow [0, +\infty)$ a function, where D_X^d denotes the diameter of X . Then (X, d) is said to have a g -embedding [[Anderes et al., 2020](#)] into a Hilbert space $(H, \|\cdot\|_H)$, written $(X, d) \xrightarrow{g} H$, if there exists a map $\psi : X \rightarrow H$ such that, for all $x, y \in X$,

$$g(d(x, y)) = \|\psi(x) - \psi(y)\|_H.$$

If g is the identity map, then it is called *isometric embedding*.

B Definition of isotropic kernels on arbitrary domains

In this brief Section, we state and enrich some crucial results of [Andres et al. \[2020\]](#) that can be used in a variety of different frameworks. While [Theorem 1](#) furnishes a straightforward recipe for the definition of kernels as compositions of variograms and completely monotone functions, [Proposition 7](#) characterises the separation property and the triangle inequality for a variogram. As a sheer application of the former, we obtain the proof of [Proposition 6](#).

Theorem 1. *Let Z be a stochastic process defined on a set X such that $\mathbb{E}(Z^2(x)) < +\infty$ for all $x \in X$. Define*

$$\begin{aligned} d : X \times X &\rightarrow \mathbb{R}_0^+ \\ (x_1, x_2) &\mapsto \gamma_Z(x_1, x_2) = \text{Var}(Z(x_1) - Z(x_2)). \end{aligned} \quad (17)$$

In addition, let ψ be a non-constant completely monotone function on $[0, +\infty)$. Then the following holds:

1. $(X, d) \xrightarrow{\sqrt{\cdot}} H$ for some Hilbert space H , that is: there exist a Hilbert space H and a function $\xi : X \rightarrow H$ such that, given $x_1, x_2 \in X$:

$$\sqrt{d(x_1, x_2)} = \|\xi(x_1) - \xi(x_2)\|_H;$$

2. the function $(x_1, x_2) \mapsto \psi(d(x_1, x_2))$ is positive semidefnite;
3. if, in addition, d is a semi-metric on X (see [Proposition 7](#) for a useful characterisation), then $(x_1, x_2) \mapsto \psi(d(x_1, x_2))$ is strictly positive definite.

Proposition 7. *Let Z , X and d as in [Theorem 1](#). Then:*

1. (X, d) is a semi-metric space if and only if, for all $x_1, x_2 \in X$, $Z(x_1) = Z(x_2)$ almost surely implies $x_1 = x_2$;
2. d satisfies the triangular inequality if and only if, for all $x_1, x_2, x_3 \in X$, it holds:

$$\text{Cov}(Z(x_1) - Z(x_2), Z(x_3) - Z(x_2)) \geq 0.$$

C Mathematical proofs

Proof of Proposition 1. From the definition of Z_V , we have that

$$\begin{aligned} \text{Cov}(Z_V(u_1), Z_V(u_2)) &= (1 - \delta_1)(1 - \delta_2) L^+[\underline{u}_1, \underline{u}_2] + (1 - \delta_1)\delta_2 L^+[\underline{u}_1, \bar{u}_2] \\ &\quad + \delta_1(1 - \delta_2) L^+[\bar{u}_1, \underline{u}_2] + \delta_1\delta_2 L^+[\bar{u}_1, \bar{u}_2] \\ &= \boldsymbol{\delta}_1^\top L^+[(\underline{u}_1, \bar{u}_1), (\underline{u}_2, \bar{u}_2)] \boldsymbol{\delta}_2. \end{aligned} \quad (18)$$

Let us now consider the process Z_E . For the sake of simplicity, here we set $e_1 := (\underline{u}_1, \bar{u}_1)$ and $e_2 := (\underline{u}_2, \bar{u}_2)$. By construction, the covariance between $Z_E(u_1)$ and $Z_E(u_2)$ is null whenever $\text{lf}(e_2) \neq \text{lf}(e_1)$. Furthermore,

$$\text{Cov}(Z_E(u_1), Z_E(u_2)) = \ell(e_1) (\min(\delta_1, \delta_2) - \delta_1\delta_2)$$

if $e_1 = e_2 \in E_T$ and

$$\text{Cov}(Z_E(u_1), Z_E(u_2)) = \sqrt{\ell(e_1)\ell(e_2)} k_T(|t(\underline{u}_1) - t(\underline{u}_2)|) (\min(\delta_1, \delta_2) - \delta_1\delta_2)$$

if $e_1, e_2 \in E_S$ and $\text{lf}(e_1) = \text{lf}(e_2)$. By noticing that the covariance expression for former case is actually a special case of the one of the latter (recall that $k_T(0) = 1$), we can summarise the covariance function of Z_E for each couple of points $u_1, u_2 \in \mathbf{G}$ as follows:

$$k_{Z_E}(u_1, u_2) = \mathbb{1}_{\text{lf}(e_1)=\text{lf}(e_2)} \sqrt{\ell(e_1)\ell(e_2)} k_T(|t(\underline{u}_1) - t(\underline{u}_2)|) (\min(\delta_1, \delta_2) - \delta_1\delta_2). \quad (19)$$

Notice that the process Z_E is defined on all the vertices V (it is zero) and that the expression (19) is meaningful even when any of the points u_1 and u_2 belongs to V . Indeed, if, say, $u_1 \in V$, then $\delta_1 \in \{0, 1\}$ regardless of which incident edge (u, v) is taken in the expression $u_1 = (u, v, \delta)$. As a consequence, the last factor in (19) vanishes and the covariance is therefore null. Finally, notice that, since Z_V and Z_E are independent, the covariance function of Z is simply the sum of (18) and (19). \square

Proof of Proposition 2. Symmetry, non-negativeness and the implication $u_1 = u_2 \implies d(u_1, u_2) = 0$ follow immediately from (7). Therefore, we just need to show that $d(u_1, u_2) = 0 \implies u_1 = u_2$. From (7), if $d(u_1, u_2) = 0$, then $Z(u_1) = Z(u_2)$ almost surely. As a consequence:

$$Z_V(u_1) - Z_V(u_2) = -Z_E(u_1) + Z_E(u_2).$$

Being Z_V and Z_E independent, necessarily $Z_V(u_1) - Z_V(u_2) = 0$ and $-Z_E(u_1) + Z_E(u_2) = 0$, hence $Z_V(u_1) = Z_V(u_2)$ and $Z_E(u_1) = Z_E(u_2)$ a.s.. Now $Z_V(u_1)$ and $Z_V(u_2)$ are linear combinations of $Z_V(V)$, that is: $Z_V(u_1) = x_1^\top Z_V(V)$ and $Z_V(u_2) = x_2^\top Z_V(V)$ for some $x_1, x_2 \in \mathbb{R}^N$, where $N = |V|$. More specifically, x_1 and x_2 have the following structure (here we assume that the vertices V are ordered, so that \underline{u}_i comes before \bar{u}_i , for $i \in \{1, 2\}$):

$$\begin{cases} x_1^\top = \begin{bmatrix} \mathbf{0}^\top & 1 - \delta_e(u_1) & \mathbf{0}^\top & \delta_e(u_1) & \mathbf{0}^\top \end{bmatrix} \\ x_2^\top = \begin{bmatrix} \mathbf{0}^\top & 1 - \delta_e(u_2) & \mathbf{0}^\top & \delta_e(u_2) & \mathbf{0}^\top \end{bmatrix}, \end{cases}$$

where the $\mathbf{0}$'s represent vectors of zeroes of the appropriate length (possibly zero). Since $Z_V(u_1) = Z_V(u_2)$ a.s., it follows that $(x_1 - x_2)^\top Z_V(V) = 0$ a.s., that is: $x_1 - x_2 = \lambda \mathbf{1}_N$ for some $\lambda \in \mathbb{R}$. Hence,

$$\lambda = \lambda \frac{\mathbf{1}_N^\top \mathbf{1}_N}{N} = \frac{1}{N} \mathbf{1}_N^\top (x_1 - x_2) = \frac{1}{N} (\mathbf{1}_N^\top x_1 - \mathbf{1}_N^\top x_2) = 0.$$

This means that $x_1 = x_2$, that is $u_1 = u_2$. □

Proof of Proposition 3. Consider the equivalent simple graph represented in Figure 4, where all the weights are 1, exception made for the edges (A_0, B_0) and A_2, B_2 , which have weights ε and $\frac{1}{\varepsilon}$ respectively, for a sufficiently small $\varepsilon > 0$. Considering the vertices in the order $A_0, B_0, A_1, \dots, B_2$, the laplacian matrix L is

$$L = \begin{bmatrix} 1 + \varepsilon & -\varepsilon & -1 & 0 & 0 & 0 \\ -\varepsilon & 1 + \varepsilon & 0 & -1 & 0 & 0 \\ -1 & 0 & 3 & -1 & -1 & 0 \\ 0 & -1 & -1 & 3 & 0 & -1 \\ 0 & 0 & -1 & 0 & 1 + \frac{1}{\varepsilon} & -\frac{1}{\varepsilon} \\ 0 & 0 & 0 & -1 & -\frac{1}{\varepsilon} & 1 + \frac{1}{\varepsilon} \end{bmatrix}.$$

Let now consider the points $P := (0, A_0, B_0, \frac{1}{2})$, $Q := (1, A_1, B_1, \frac{1}{2})$ and $R := (2, A_2, B_2, \frac{1}{2})$. We will show that, for any $\gamma > 0$, for ε sufficiently small, it holds

$$d(P, Q) + d(Q, R) < d(P, R). \quad (20)$$

First, let us rewrite and simplify a bit (20). Notice that here all the δ 's are $\frac{1}{2}$.

$$\begin{aligned}
(20) &\iff k_Z(P, P) + k_Z(Q, Q) - 2k_Z(P, Q) \\
&\quad + k_Z(Q, Q) + k_Z(R, R) - 2k_Z(Q, R) \\
&\quad < k_Z(P, P) + k_Z(R, R) - 2k_Z(P, R) \\
&\iff k_Z(Q, Q) - k_Z(P, Q) - k_Z(Q, R) < -k_Z(P, R) \\
&\iff \frac{1}{4} \mathbf{1}_2^\top L^+ [(A_1, B_1), (A_1, B_1)] \mathbf{1}_2 + \sqrt{1 \cdot 1} \gamma^0 \cdot \frac{1}{4} \\
&\quad - \frac{1}{4} \mathbf{1}_2^\top L^+ [(A_0, B_0), (A_1, B_1)] \mathbf{1}_2 - \sqrt{\frac{1}{\varepsilon} \cdot 1} \gamma^1 \cdot \frac{1}{4} \\
&\quad - \frac{1}{4} \mathbf{1}_2^\top L^+ [(A_1, B_1), (A_2, B_2)] \mathbf{1}_2 - \sqrt{1 \cdot \varepsilon} \gamma^1 \cdot \frac{1}{4} \\
&\quad < -\frac{1}{4} \mathbf{1}_2^\top L^+ [(A_0, B_0), (A_2, B_2)] \mathbf{1}_2 - \sqrt{\frac{1}{\varepsilon} \cdot \varepsilon} \gamma^2 \cdot \frac{1}{4} \\
&\iff \mathbf{1}_2^\top (L^+ [(A_1, B_1), (A_1, B_1)] + L^+ [(A_0, B_0), (A_2, B_2)]) \mathbf{1}_2 \\
&\quad + \mathbf{1}_2^\top (-L^+ [(A_0, B_0), (A_1, B_1)] - L^+ [(A_1, B_1), (A_2, B_2)]) \mathbf{1}_2 \\
&\quad < -1 + \frac{\gamma}{\sqrt{\varepsilon}} + \gamma\sqrt{\varepsilon} - \gamma^2. \tag{21}
\end{aligned}$$

Notice that the right-hand size of the last inequality (21) is not limited for any $\gamma > 0$ when $\varepsilon \rightarrow 0^+$. As a consequence, it is sufficient to show that the left-hand size is limited when $\varepsilon \rightarrow 0^+$. Indeed the left-hand side of the last inequality is a sheer signed sum of 16 elements of the matrix L^+ . This sum is surely not greater than

$$16 \max_{i,j \in \{1, \dots, 6\}} |L^+[i, j]| \leq 16 \max_{i \in \{1, \dots, 6\}} |L^+[i, i]|.$$

Now, in our case, the main diagonal of L^+ is given by:

$$\text{diag}(L^+) = \begin{bmatrix} \frac{10\varepsilon^2 + 39\varepsilon + 34}{36(\varepsilon^2 + 3\varepsilon + 1)}, \frac{10\varepsilon^2 + 39\varepsilon + 34}{36(\varepsilon^2 + 3\varepsilon + 1)}, \frac{10\varepsilon^2 + 27\varepsilon + 10}{36(\varepsilon^2 + 3\varepsilon + 1)}, \frac{10\varepsilon^2 + 27\varepsilon + 10}{36(\varepsilon^2 + 3\varepsilon + 1)}, \\ \frac{34\varepsilon^2 + 39\varepsilon + 10}{36(\varepsilon^2 + 3\varepsilon + 1)}, \frac{34\varepsilon^2 + 39\varepsilon + 10}{36(\varepsilon^2 + 3\varepsilon + 1)} \end{bmatrix}.$$

As all the entries are continuous functions of $\varepsilon \in [0, 1]$, they are limited. Since the maximum of (a finite number of) limited functions on the same domain is limited, the left-hand of (21) is limited as well. This concludes the proof. \square

Proof of Proposition 5. The proof is very similar to the one of Proposition 2. Also in this case, we get symmetry, non-negativeness and the implication $u_1 = u_2 \implies d(u_1, u_2) = 0$ immediately from (7). Let us show that $d(u_1, u_2) = 0 \implies u_1 = u_2$. From (7), if $d(u_1, u_2) = 0$, then $Z(u_1) = Z(u_2)$ almost surely. As a consequence:

$$Z_V(u_1) - Z_V(u_2) = -Z_E(u_1) + Z_E(u_2) - \beta W(t_1) + \beta W(t_2).$$

Since Z_V is independent from Z_E and W , it must be $Z_V(u_1) = Z_V(u_2)$ a.s.. Following the same argument of the proof of Proposition 2, we obtain $(\underline{u}_1, \bar{u}_1, \delta_1) = (\underline{u}_2, \bar{u}_2, \delta_2)$. It remains to be shown that $t_1 = t_2$. Again, using $Z(u_1) = Z(u_2)$, and the independence between W_t and both Z_V and Z_E , we obtain $\beta W(t_1) = \beta W(t_2)$ a.s., that is $t_1 = t_2$. \square

Proof of Theorem 1. 1. Define $\tilde{d} := \sqrt{d}$. Since $d = \tilde{d}^2$ is a variogram, it is conditionally negative semidefinite: as a consequence, by Anderes et al. [2020, Theorem 6], $(X, \tilde{d}) \xrightarrow{id} H$ for some Hilbert space H . Therefore $(X, d) \xrightarrow{\sqrt{\cdot}} H$.

2. Follows immediately from the previous point and Anderes et al. [2020, Corollary 1].
3. If $Z(x_1) = Z(x_2)$ almost surely implies $x_1 = x_2$, then (X, d) is a semi-metric space by Proposition 7. Thus, by Anderes et al. [2020, Corollary 1], $(x_1, x_2) \mapsto C(d(x_1, x_2))$ is strictly positive definite. \square

Proof of Proposition 7. 1. (X, d) is a semi-metric space iff $d(x_1, x_2) = 0$ implies $x_1 = x_2$. But $d(x_1, x_2) = 0$ is equivalent to $Z(x_1) = Z(x_2)$ almost surely.

2. Without loss of generality, we can restrict the proof to a zero-mean process X . Indeed, both the variance and the covariance do not change if we change the mean of their arguments. The proof consists in the

following chain of equivalences. Let $x_1, x_2, x_3 \in X$.

$$\begin{aligned}
& d(x_1, x_2) + d(x_2, x_3) \geq d(x_1, x_3) \\
\iff & \mathbb{V}\text{ar} (Z(x_1) - Z(x_2)) + \mathbb{V}\text{ar} (Z(x_2) - Z(x_3)) \geq \mathbb{V}\text{ar} (Z(x_1) - Z(x_3)) \\
\iff & \mathbb{V}\text{ar} Z(x_1) + \mathbb{V}\text{ar} Z(x_2) - 2 \mathbb{C}\text{ov} (Z(x_1), Z(x_2)) \\
& \quad + \mathbb{V}\text{ar} Z(x_2) + \mathbb{V}\text{ar} Z(x_3) - 2 \mathbb{C}\text{ov} (Z(x_2), Z(x_3)) \geq \\
& \quad \mathbb{V}\text{ar} Z(x_1) + \mathbb{V}\text{ar} Z(x_3) - 2 \mathbb{C}\text{ov} (Z(x_1), Z(x_3)) \\
\iff & \mathbb{V}\text{ar} Z(x_2) - \mathbb{C}\text{ov} (Z(x_1), Z(x_2)) - \mathbb{C}\text{ov} (Z(x_2), Z(x_3)) \geq \\
& \quad - \mathbb{C}\text{ov} (Z(x_1), Z(x_3)) \\
\iff & \mathbb{E} (Z^2(x_2) + Z(x_1)Z(x_3) - Z(x_1)Z(x_2) - Z(x_2)Z(x_3)) \geq 0 \\
\iff & \mathbb{E} ((Z(x_2) - Z(x_1))(Z(x_2) - Z(x_3))) \geq 0 \\
\iff & \mathbb{C}\text{ov} (Z(x_2) - Z(x_1), Z(x_2) - Z(x_3)) \geq 0
\end{aligned}$$

□